Design and Adaptation of Multi-Interference Steering

Zhao Li, *Member, IEEE*, Yinghou Liu, Kang G. Shin, *Life Fellow, IEEE*, Jun Li, Fengjuan Guo, and Jia Liu, *Member, IEEE*

***Abstract*— With the rapid development in wireless communication technologies, interference has become a main impediment to network performance, making interference management (IM) a critical issue. Interference steering (IS) is emerging as a novel way of IM, which can steer the spatial feature of interference to a target subspace by exploiting the interactions of multiple signals over the air to avoid the disturbance to the interfered receiver. In reality, there always exists multiple interferences from single or multiple sources. We propose three ways to realize IS. The first two of them are categorized as *individual interference steering* (IIS), in which multiple interfering signals are separately adjusted to either an identical direction (*a single-target IS*, STIS) or different directions (*multi-target IS*, MTIS), incurring single or multiple degrees of freedom (DoFs) overheads, respectively. Furthermore, by recognizing that the goal of IM is to limit the effect of interference—i.e., the effective portion of interference imposed on the intended transmission— we propose *aggregated interference steering* (AIS) that exploits the constructive or destructive effects of multiple interfering signals. By considering the overall effect of multiple interferences, the DoF cost of AIS is reduced to one regardless of the number of interference to be managed. Finally, the proposed three IS realizations are adapted to minimize the power cost of steering interference. Our theoretical analysis and in-depth simulation results have shown that the proposed IS schemes can effectively manage multiple interference via better utilizing the DoF and transmit power. The AIS is shown to be advantageous in both power cost and DoF consumption.**

Manuscript received January 3, 2018; revised July 4, 2018, November 15, 2018 and February 28, 2019; accepted March 20, 2019. Date of publication April 23, 2019; date of current version July 10, 2019. This work was supported in part by the China 111 Project under Grant B16037, in part by the Fundamental Research Funds for the Central Universities under Grant JB171503, in part by NSFC under Grant 61672410 and Grant 61802292, in part the Project of Cyber Security Establishment with Inter University Cooperation, in part by the Secom Science and Technology Foundation, and in part by the U.S. National Science Foundation under Grant CNS-1317411. The associate editor coordinating the review of this paper and approving it for publication was G. C. Alexandropoulos. *(Corresponding author: Zhao Li.)*

Z. Li is with the School of Cyber Engineering, Xidian University, Xi'an 710126, China, also with the Shaanxi Key Laboratory of Information Communication Network and Security, Xi'an University of Posts and Telecommunications, Xi'an 710121, China, and also with the School of Information Engineering, Eurasia University, Xi'an 710065, China (e-mail: zli@xidian.edu.cn).

Y. Liu and F. Guo are with the School of Telecommunications Engineering, Xidian University, Xi'an 710071, China.

K. G. Shin is with the Department of Electrical Engineering and Computer Science, The University of Michigan, Ann Arbor, MI 48109-2121 USA.

J. Li is with the School of Cyber Engineering, Xidian University, Xi'an 710071, China.

J. Liu is with the Center for Cybersecurity Research and Development, National Institute of Informatics, Tokyo 101-8430, Japan.

Color versions of one or more of the figures in this paper are available online at http://ieeexplore.ieee.org.

Digital Object Identifier 10.1109/TWC.2019.2908158

***Index Terms*— Multi-antenna system, interference steering, degree of freedom, costs, adaptive signal processing.**

I. Introduction

With the rapid development of wireless communication technologies as well as the increasing density of link connectivity, interference has become a major impediment in network performance. Therefore, given limited resources, effective interference management (IM) is crucial to the ever-increasing demand of users' Quality of Service (QoS) and the increasing number of users accommodated in the system. IM can be implemented at the transmitter (Tx) and/or the receiver (Rx) side. There have been numerous IM schemes, such as zero-forcing beamforming (ZFBF) [1], ZF reception [2], interference alignment (IA) [3]–[7], interference neutralization (IN) [9]–[14], and interference steering (IS) [15]. They are all designed to suppress, adjust or eliminate interference so as to improve network capacity and users' experience.

Of these IM schemes, IA is powerful in controlling the interference contamination and has been under development in recent years [3]–[7]. By pre-processing them at the Tx, multiple interfering signals are mapped into a finite subspace, so that the desired signal(s) may be sent through a subspace without attenuation [3], [4]. IA has been shown to be able to achieve the information-theoretic maximum DoFs (Degrees of Freedom) in some interference networks [5], [6]. However, the authors of [3] have shown that the feasibility of IA is highly dependent on system parameters, such as the number of transmitters and receivers and configuration of transmit/receive antennas. That is, although IA emerges as a promising IM scheme, its applicability is still limited by the requirement of DoFs. Moreover, with IA, signals from an identical Tx cannot be aligned in the same direction at an unintended Rx while being distinguishable at their common destination [8].

Some researchers have attempted to bypass the stringent DoFs requirement by proposing other IM schemes, such as interference neutralization (IN) [9]–[14]. IN strives to properly combine signals arriving from various paths in such a way that the interfering signals are canceled while the desired signals are preserved at the receiver [9], and it has been applied to interference networks that employ relays [10], [11]. The authors of [12] proposed a new scheme called aligned interference neutralization for a multi-hop interference network formed by concatenation of two 2-user interference channels. It provides a way to align interference terms over

each hop in a manner that allows them to be canceled over the air at the last hop. But a conventional relay causes a processing delay compared to the direct path between a source and destination, which limits the DoF gain in a wireless interference network [13], [14]. Therefore, instantaneous relay (relay-without-delay) was introduced in [13], [14] to obtain larger capacity than conventional relay, and a higher DoF gain is achieved without requiring any memory at the relay.

Although IN can mitigate interference, the power overhead of generating neutralizing signal influences the system's performance as well. In practice, a higher transmit power will be consumed by IN when the interference is strong, thus leaving less power for the desired data transmission. Furthermore, IN may even be unavailable for mobile terminals due to their limited power budget. A dynamic interference neutralization (DIN) scheme was proposed in [8]. By intelligently determining the appropriate portion of interference to be neutralized, the transmitter's power used for IN and the desired signal's transmission can be well balanced. Although DIN achieves better use of transmit power compared to complete IN, its power overhead is still dependent on the strength of interference.

Recently, by recognizing that interference can be not only neutralized but also steered to a particular direction [15], a new IM technique called interference steering (IS) was proposed and applied to an infrastructure-based enterprise wireless local area network (WLAN). With IS, a steering signal is generated to modify the interference's spatial feature, so that the original interference is steered to the orthogonal direction of the desired signal perceived by the interfered receiver. Compared to IN, IS consumes much less transmit power [15], yet a spatial DoF is required to place the steered interference which is similar to the principle of IA.

Besides the above-mentioned methods, optimal beamforming (OBF) is also an effective way of managing multi-user interference in multiple-input multiple-output broadcast channel (MIMO BC). Of these, [16]–[20] focused on the practical design of beamforming strategies, i.e., designing transmit vectors under limited feedback [16], [19], [20], statistical channel state information (CSI) [17], [18], and delayed CSI [18], so that the ergodic sum-rate can be maximized.

Note, however, that none of the existing IM methods are cost-free when being used to adjust, suppress or eliminate the interference. For example, by adjusting a transmit beam using ZFBF, OBF, or IA to implement interference management, the strength of the adjusted signal is attenuated; a zero-forcing based filter can be adopted to nullify interference at a loss of the desired signal power; with IN or IS, an interfering signal is duplicated to neutralize or steer the interference at the cost of extra transmit power consumption. Moreover, given multiple mutually interfering transmission pairs, ZFBF, OBF, ZF reception, IA and IS require more DoFs than IN, to distinguish the desired signal from the interference. For ZFBF, OBF and ZF reception, the DoF requirement is determined by the total number of desired signals and interference, i.e., each interfering signal component consumes one DoF, whereas for IA and IS at least one DoF should be provided to place the aligned and steered interference, respectively. With IN, since disturbance(s) can be neutralized over the air, no extra DoF for interference is required, thus becoming free from the aforementioned limitations of ZFBF, OBF, ZF reception, IA and IS. To better utilize the transmit power used for IM and desired signal's transmission, the authors of [21] proposed dynamic interference steering (DIS). As for ZF, IM is implemented by the interfered Rx, whereas IN and IS are realized by the interfered Tx (the transmitter corresponding to the interfered receiver), thus incurring effective signal power loss with respect to the interfered user-pair. With ZFBF and IA, the IM cost is paid by the interfering Tx, hence incurring effective signal power loss with respect to the interfering user-pair. However, in practice, when the interferer is unwilling to sacrifice, ZFBF and IA become inapplicable. In addition, compared to IN and IS, the realization of ZF costs more DoFs.

Note that the above discussion is under the assumption of existence of multiple mutually interfering transmission pairs, thus making the OBF designed for MIMO BC inapplicable. If MIMO BC is considered, we do not need multi-antennas at the Rx side for the application of ZFBF and OBF, hence no DoF cost at the interfered Rx. Moreover, since there is one common Tx and multiple Rxs in MIMO BC, the transmission from Tx to the intended Rx is not only desired for itself but also the interfering transmission to the other Rxs, thus incurring power loss to both the interfering and interfered transmissions.

Based on the above discussion, IS and DIS are advantageous over ZF in DoF cost and IN in power overhead, respectively. Moreover, IS and DIS are implemented by the interfered Tx and does not require the sacrifice of interfering user-pair's performance. Thus, IS and DIS are more attractive than other IM methods. However, existing IS and DIS schemes manage only a single interference, even when there are multiple interfering signals from single/multiple sources. In addition, as one can see from the above discussion, power and DoF costs are two major types of overhead in the design of IM mechanisms (including IS), but neither [15] nor [21] discussed the DoF cost of managing multiple disturbances. Moreover, the above-mentioned IM schemes focus on managing disturbances individually, but have not exploited interactions among multiple disturbances for the design of IM.

In summary, how to flexibly utilize various types of communication resource such as transmit power and DoF so as to manage multiple disturbances effectively, and in which way to manage multiple interferences (i.e., individually or in an aggregated way) are important and require a thorough investigation. So, we will focus on the design of various IS schemes in the presence of multiple disturbances, and analyze their overheads based on which their adaptation will be discussed to better utilize the DoFs and power for IM.

The main contributions of this paper are three-fold:

- Proposal of two types of individual interference steering (IIS), with which each interfering signal is steered separately. By accounting for the transmitter power consumption and DoF cost, multiple interferences can be steered in different directions or an identical direction, which are regarded as *multi-target IS* (MTIS) and *single-target IS* (STIS), respectively. MTIS can save transmit

power at the expense of more DoF costs, compared to STIS.

- Proposal of *aggregated IS* (AIS), with which the inter-relationship of transmitted symbols carried by multiple interfering signals is exploited so that a single steering signal can be generated to adjust the overall effect of the interference perceived by the interfered Rx to the direction orthogonal to the desired transmission. AIS consumes only one DoF (antenna) regardless of the number of interference. Moreover, by exploiting interactions among interference, the power overhead of generating a steering signal with AIS can be reduced further.
- Adaptation of the proposed IS schemes, with which the DoF and transmit power can be appropriately utilized so as to maximize the interfered user-pair's spectral efficiency (SE).

The rest of this paper is organized as follows. Section II describes the system model, while Section III details the individual interference steering (IIS). Section IV presents the aggregated IS (AIS) and the adaptive selection of IS schemes. Then, Section V generalizes the three IS implementations. Section VI analyzes the computational complexity of the proposed methods, and Section VII evaluates their performance and overheads. Finally, Section VIII concludes the paper.

Throughout this paper, we use the following notations. The set of complex numbers is denoted as $\mathbb{C}$, while vectors and matrices are represented by bold lower-case and upper-case letters, respectively. Let $\mathbf{X}^H$, $\mathbf{X}^T$, $\mathbf{X}^{-1}$, $\det(\mathbf{X})$ denote the Hermitian, transpose, inverse and determinant of matrix $\mathbf{X}$. $\|\cdot\|$ and $|\cdot|$ indicate the Euclidean norm and the absolute value, respectively. $\mathbb{E}(\cdot)$ denotes statistical expectation and $\langle \mathbf{a}, \mathbf{b} \rangle$ represents the inner product of two vectors.

II. System Model

We consider the downlink transmission in heterogeneous cellular networks (HCNs) composed of overlapping macro and pico cells [22]. As shown in Fig. 1, macro and pico base stations (MBSs and PBSs) are equipped with N_{T_1} and N_{T_0} antennas, whereas macro user equipment (MUE) and pico user equipment (PUE) have N_{R_1} and N_{R_0} antennas, respectively. Since mobile stations/devices are subject to more severe restrictions in cost and hardware than a base station (BS), the number of BS's antennas is assumed to be equal to, or greater than the number of UE's antennas, i.e., $N_{T_i} \geq N_{R_i}$ where $i = 0, 1$. The radio range, d, of a picocell is known to be 300m or less, whereas the radius, D, of a macrocell is taken 3000m [22]. Symbols $\mathbf{x}_1 = [x_1^{(1)}\ x_1^{(2)}\ \cdots\ x_1^{(K)}]^T$ and $\mathbf{x}_0 = [x_0^{(1)}\ x_0^{(2)}\ \cdots\ x_0^{(M)}]^T$ are used to denote the transmit data vectors from PBS and MBS to their serving subscribers, respectively, of which $x_1^{(k)}$ ($k \in \{1, 2, \cdots, K\}$ and $K \leq N_{R_1}$) and $x_0^{(m)}$ ($m \in \{1, 2, \cdots, M\}$ and $M < N_{R_0}$, $N_{R_0} - M$ represents for the DoF costs available for IM) are the k^{th} and m^{th} symbols. $\mathbb{E}(\|\mathbf{x}_i\|^2) = 1$ holds. For clarity of exposition, we begin with the assumption that multiple data streams are sent from MBS to MUE ($K > 1$), and only one data stream is sent from PBS to PUE ($M = 1$), i.e., spatial multiplexing (SM) and beamforming (BF) are employed by MBS and PBS, respectively. The extension to multiple data streams sent from PBS and other generalized situations will be described in Section V.

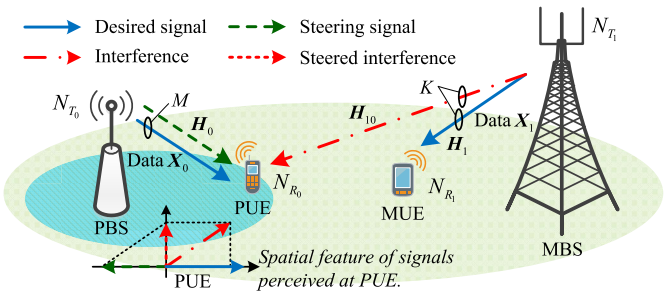

Fig. 1. System model.

Let P_{T_1} and P_{T_0} be the transmit power of MBS and PBS. The path loss from MBS and PBS to a mobile terminal is defined as $L_{10} = \mathcal{F}(\eta_{10})$ and $L_0 = \mathcal{F}(\eta_0)$, respectively, where the variables η_{10} and η_0, measured in meters (m), denote the distance from the transmitter to the receiver. That is, path loss is a function — i.e., $\mathcal{F}(\cdot)$ — of the signal's propagation distance. Here we adopt the Third Generation Partnership Project (3GPP) path loss model [23] as an example, but our proposed methods can be directly applied to other models. Channel matrices from MBS to MUE and from PBS to PUE are denoted by $\mathbf{H}_1 \in \mathbb{C}^{N_{R_1} \times N_{T_1}}$ and $\mathbf{H}_0 \in \mathbb{C}^{N_{R_0} \times N_{T_0}}$, whereas from MBS to PUE is expressed as $\mathbf{H}_{10} \in \mathbb{C}^{N_{R_0} \times N_{T_1}}$. A spatially uncorrelated Rayleigh flat fading channel model is adopted so as to model the elements of the above matrices as independent and identically distributed zero-mean unit-variance complex Gaussian random variables. We assume that all users experience block fading, i.e., channel parameters in a block consisting of several successive time slots remain constant in the block and vary randomly between successive blocks. Each user can accurately estimate CSI with respect to its intended and unintended Txs and feed it back to its associated BS via a low-rate error-free link. We assume reliable links for the delivery of CSI and signaling (as is usually the case in practice). The delivery delay is negligible relative to the time scale on which the channel state varies.

As mobile data traffic has increased significantly in recent years, network operators prefer open access to offload users' traffic from heavily-loaded macrocells to other low-power access points, e.g., pico BS [22], [24]. Hence, in this paper we assume the PBS operates in an open mode, i.e., users falling into the coverage of PBS are allowed to access it. The transmission from MBS to MUE will interfere with the intended transmission from PBS at PUE. Nevertheless, due to the limited coverage of a picocell, PBS will not cause too much interference to MUE, and thus is omitted in our study. Therefore, the interference shown in Fig. 1 has an asymmetric feature. According to the above description, MBS and PUE act as the interfering Tx and the interfered Rx, and MUE and PBS, corresponding to the interfering Tx and interfered Rx, will henceforth be called interfering Rx and the interfered Tx, respectively.

Since picocells are deployed to improve the capacity and coverage of existing cellular systems, each picocell, unlike the macrocell, has subordinate features,[1] and hence the transmission in the macrocell is given priority over that in the picocell. Specifically, the MBS is unwilling to adjust its transmission for the pico-users. However, we assume that PBS can acquire the information of $\mathbf{x}_1$ via inter-BS collaboration, this is easy to achieve because PBS and MBS are deployed and managed by the same operator [25]. Moreover, we assume that PUE deployed in the coverage of a macrocell can hear the training signal broadcasted by MBS so that the interfering channel matrix $\mathbf{H}_{10}$ can be estimated by the PUE. Then, $\mathbf{H}_{10}$ is fed back to PBS along with $\mathbf{H}_0$. Since the transmission from MBS to MUE depends only on $\mathbf{H}_1$ and is free from interference, we mainly focus on the pico-users' transmission performance.

III. Design of Individual Interference Steering

When there are $K \geq 2$ disturbances, IS can be realized by generating a steering signal in terms of each of the interference, called *individual IS* (IIS). Two types of IIS can be obtained at different DoF costs. Given $N_{R_0} - M > 1$, when K interfering signals are independently steered to various directions, as many as $\min(N_{R_0} - M, K)$ DoFs are consumed to place the adjusted interference, we call it *multi-target IS* (MTIS). When all interfering signals are adjusted to an identical direction, one DoF is consumed by the interference at the interfered Rx, we call it *single-target IS* (STIS). For clarity of exposition, we start with one interfering MBS who sends $\mathbf{x}_1 = [x_1^{(1)} \ \cdots \ x_1^{(K)}]$ where $K > 1$ and $N_{T_i} = N_{R_i} > 2$ $(i = 0, 1)$. PBS employs BF to transmit $x_0^{(1)}$ to PUE. Note that our design can be easily extended to more generalized cases where interfering signals come from multiple sources. In what follows, we will first elaborate on the design of MTIS and STIS, and then analyze the power overhead of the two schemes.

A. Design of Multi-Target IS

As mentioned above, there are K disturbances from the interfering MBS, and thus the received signal at the interfered PUE can be expressed as:

$$\mathbf{y}_0 = \sqrt{P_{T_0}} 10^{-0.05 L_0} \mathbf{H}_0 \mathbf{p}_0^{(1)} x_0^{(1)} + \sum_{k=1}^{K} \sqrt{\frac{P_{T_1}}{K}} 10^{-0.05 L_{10}} \mathbf{H}_{10} \mathbf{p}_1^{(k)} x_1^{(k)} + \mathbf{n}_0. \tag{1}$$

The column vectors $\mathbf{p}_0^{(1)}$ and $\mathbf{p}_1^{(k)}$ where $k = 1, 2, \ldots, K$, denote the precoders for data symbols $x_0^{(1)}$ and $x_1^{(k)}$ sent from PBS and MBS, respectively. The first term on the right hand side (RHS) of Eq. (1) is the desired signal of PUE, whereas the second term denotes the sum of interference from MBS. P_{T_1} is equally allocated to K data streams. $\mathbf{n}_0$ represents for an additive white Gaussian noise (AWGN) with zero-mean and variance σ_n^2. The path losses from MBS and PBS to a mobile terminal are denoted by L_{10} and L_0, measured in dB, respectively. For example, by employing the path loss model in [23], we can have $L_{10} = 128.1 + 37.6 \log_{10}(\eta_{10}/10^3)$ dB and $L_0 = 38 + 30 \log_{10} \eta_0$ dB, where η_{10} and η_0 are the distances from MBS and PBS to PUE, respectively. From Fig. 1, we can see that the strengths of the desired signal and interference at PUE depend on the network topology, transmit power of PBS and MBS, as well as channel conditions. All of these factors affect the effectiveness of IM. For clarity of presentation, we define $\tilde{P}_{T_0} = P_{T_0} 10^{-0.1 L_0}$ and $\tilde{P}_{T_1} = P_{T_1} 10^{-0.1 L_{10}}$, where $\tilde{P}_{T_0}$ and $\tilde{P}_{T_1}$ indicate the transmit power of PBS and MBS incorporated in path loss. With this definition, the consideration of various network topology and transmit power differences can be simplified to $\tilde{P}_{T_0}$ and $\tilde{P}_{T_1}$.

We adopt the precoding and receive filtering based on the singular value decomposition (SVD), but can also use other types of pre- and post-processing. By applying SVD to $\mathbf{H}_i$ where $i = 0, 1$, $\mathbf{H}_i = \mathbf{U}_i \mathbf{\Sigma}_i \mathbf{V}_i^H$ is obtained. Then, we employ $\mathbf{p}_0^{(1)} = \mathbf{v}_0^{(1)}$ and $\mathbf{p}_1^{(k)} = \mathbf{v}_1^{(k)}$, where $\mathbf{v}_i^{(1)}$ represents for the first column vector of the right singular matrix $\mathbf{V}_i$, corresponding to the principal eigenmode of $\mathbf{H}_i$, and $\mathbf{v}_1^{(k)}$ $(k = 2, 3, \ldots, K)$ is the k^{th} column vector of $\mathbf{V}_1$, indicating the spatial feature of the k^{th} eigenmode of $\mathbf{H}_1$. We can simply use $\mathbf{f}_0^{(1)} = \mathbf{u}_0^{(1)}$ as the filter vector at PUE, following the idea of reception based on matched filtering (MF), where $\mathbf{u}_0^{(1)}$ is the first column vector of the left singular matrix $\mathbf{U}_0$.

The above discussion is under $M = 1$ assumption. Given an arbitrary $M < N_{R_0}$, since M data streams consume M DoFs at the PUE, there will be $N_{R_0} - M$ DoFs available to place the steered interference. If $N_{R_0} - M > 1$, MTIS can be realized by applying IS to the interference K times. The steered K disturbances will lie in the subspace orthogonal to the desired transmission. The dimension of such a subspace is determined by $N_{R_0} - M$. Since PBS is capable of acquiring interference information, including data and CSI, it can generate a steering signal in terms of each interference and send it along with the desired signal. With MTIS, the received signal at PUE becomes:

$$\mathbf{y}_0 = \sqrt{\tilde{P}_{T_0} - \sum_{k=1}^{K} \tilde{P}_{MTIS}^{(k)}} \mathbf{H}_0 \mathbf{p}_0^{(1)} x_0^{(1)} + \sum_{k=1}^{K} \left[\sqrt{\frac{\tilde{P}_{T_1}}{K}} \mathbf{H}_{10} \mathbf{p}_1^{(k)} x_1^{(k)} + \sqrt{\tilde{P}_{MTIS}^{(k)}} \mathbf{H}_0 \mathbf{p}_{MTIS}^{(k)} x_1^{(k)} \right] + \mathbf{n}_0 \tag{2}$$

where $\tilde{P}_{MTIS}^{(k)} = P_{MTIS}^{(k)} 10^{-0.1 L_0}$. $P_{MTIS}^{(k)}$ and $\mathbf{p}_{MTIS}^{(k)}$ denote the power overhead and precoder of steering signal for the k^{th} interference $\sqrt{\frac{\tilde{P}_{T_1}}{K}} \mathbf{H}_{10} \mathbf{p}_1^{(k)} x_1^{(k)}$. With the influence of the steering signal, the spatial features of the original interference perceived by the interfered Rx can be modified.

Given K interfering signals, we first define the directions of the desired signal $\mathbf{s}$ and the k^{th} interference,

$$\mathbf{t}^{(k)} = \sqrt{\frac{\tilde{P}_{T_1}}{K}} \mathbf{H}_{10} \mathbf{p}_1^{(k)} x_1^{(k)}, \tag{3}$$

[1] Picocells are employed to assist a macrocell to improve its service, while MBS does not necessarily adjust its transmission, or sacrifice its communication performance to avoid interference to PUE.

combined with the steering signal,

$$\mathbf{s}_{t,MTIS}^{(k)} = \sqrt{\tilde{P}_{MTIS}^{(k)}}\mathbf{H}_0\mathbf{p}_{MTIS}^{(k)}x_1^{(k)}, \tag{4}$$

as

$$\mathbf{d_s} = \frac{\mathbf{H}_0\mathbf{p}_0^{(1)}}{\|\mathbf{H}_0\mathbf{p}_0^{(1)}\|} \tag{5}$$

and

$$\mathbf{d}_{\mathbf{t}^{(k)}+\mathbf{s}_{t,MTIS}^{(k)}} = \frac{\mathbf{t}^{(k)}+\mathbf{s}_{t,MTIS}^{(k)}}{\|\mathbf{t}^{(k)}+\mathbf{s}_{t,MTIS}^{(k)}\|}, \tag{6}$$

respectively. Then, by letting $\langle \mathbf{d_s}, \mathbf{d}_{\mathbf{t}^{(k)}+\mathbf{s}_{t,MTIS}^{(k)}} \rangle = 0$, the interference can be steered to the orthogonal direction to the desired signal. Since the interference $\mathbf{t}^{(k)}$ can be decomposed into an in-phase component and a quadrature component, denoted by the superscripts In and Q, respectively, in terms of $\mathbf{d_s}$, i.e., $\mathbf{t}^{(k)} = \mathbf{t}_{In}^{(k)} + \mathbf{t}_{Q}^{(k)}$, when $\mathbf{s}_{t,MTIS}^{(k)} = -\mathbf{t}_{In}^{(k)}$ holds for every $k \in \{1, 2, \cdots, K\}$, MTIS is realized. Taking the steering of $\mathbf{t}^{(k)}$ as an example, we can easily see

$$\mathbf{t}_{In}^{(k)} = \sqrt{\frac{\tilde{P}_{T_1}}{K}}\mathbf{P}_{MTIS}\mathbf{H}_{10}\mathbf{p}_1^{(k)}x_1^{(k)} \tag{7}$$

where $\mathbf{P}_{MTIS} = \mathbf{d_s}(\mathbf{d_s}^H\mathbf{d_s})^{-1}\mathbf{d_s}^H = \mathbf{d_s}\mathbf{d_s}^H/\|\mathbf{d_s}\|^2 = \mathbf{d_s}\mathbf{d_s}^H$ denotes the projection matrix with respect to $\mathbf{d_s}$. The steering signal should satisfy

$$\sqrt{\tilde{P}_{MTIS}^{(k)}}\mathbf{H}_0\mathbf{p}_{MTIS}^{(k)}x_1^{(k)} = -\sqrt{\frac{\tilde{P}_{T_1}}{K}}\mathbf{P}_{MTIS}\mathbf{H}_{10}\mathbf{p}_1^{(k)}x_1^{(k)}. \tag{8}$$

This equation can be decomposed into two parts,

$$\mathbf{H}_0\mathbf{p}_{MTIS}^{(k)} = -\omega_1\mathbf{P}_{MTIS}\mathbf{H}_{10}\mathbf{p}_1^{(k)} \tag{9}$$

and

$$\sqrt{\tilde{P}_{MTIS}^{(k)}} = \omega_2\sqrt{\frac{\tilde{P}_{T_1}}{K}} \tag{10}$$

where $\omega_1\omega_2 = 1$. From the above two equations, we can obtain

$$\mathbf{p}_{MTIS}^{(k)} = -\omega_1\mathbf{H}_0^{-1}\mathbf{P}_{MTIS}\mathbf{H}_{10}\mathbf{p}_1^{(k)} \tag{11}$$

and

$$\sqrt{P_{MTIS}^{(k)}} = \omega_2\sqrt{\frac{P_{T_1}\varepsilon}{K}}, \tag{12}$$

respectively, where $\varepsilon = 10^{-0.1(L_{10}-L_0)}$. Note that $\|\mathbf{p}_{MTIS}^{(k)}\| = 1$ is not guaranteed, i.e., $\mathbf{p}_{MTIS}^{(k)}$ has an impact on the power cost of interference steering. From the above discussion, it can be seen that with MTIS, the projection of each interfering signal onto the desired signal is counteracted by its corresponding steering signal, so that the adjusted interference is orthogonal to the desired signal. However, the orthogonality among the steered interference is neither necessary nor guaranteed. The spatial feature of the steering signal is determined only by the desired signal and the interference it is to adjust.

For clarity of exposition, we normalize the precoder so that the direction and strength requirements for MTIS could be decoupled from each other. Then, the implementation of MTIS is given as:

$$\begin{cases} \mathbf{p}_{MTIS}^{(k)} = -\dfrac{\mathbf{H}_0^{-1}\mathbf{P}_{MTIS}\mathbf{H}_{10}\mathbf{p}_1^{(k)}}{\|\mathbf{H}_0^{-1}\mathbf{P}_{MTIS}\mathbf{H}_{10}\mathbf{p}_1^{(k)}\|} \\ P_{MTIS}^{(k)} = \dfrac{P_{T_1}\varepsilon}{K}\|\mathbf{H}_0^{-1}\mathbf{P}_{MTIS}\mathbf{H}_{10}\mathbf{p}_1^{(k)}\|^2 \end{cases} \tag{13}$$

where $k = 1, 2, \ldots, K$. When $N_{T_i} > N_{R_i}$, the inverse of channel matrix should be replaced by Moore-Penrose pseudo-inverse. The mechanism can then be directly generalized. In addition, when the interference is too strong, P_{T_0} may not be sufficient for MTIS, in such a case, we simply switch to the non-interference management (non-IM) mode. That is, the interfered Rx employs MF to decode its desired data while leaving the interference un-managed. By adopting MF, i.e., letting $\mathbf{f}_0^{(1)} = \mathbf{u}_0^{(1)}$, the estimated signal at PUE after filtering is

$$\bar{y}_0 = \sqrt{\tilde{P}_{T_0} - \sum_{k=1}^{K}\tilde{P}_{MTIS}^{(k)}}[\mathbf{f}_0^{(1)}]^H\mathbf{H}_0\mathbf{p}_0^{(1)}x_0^{(1)} + [\mathbf{f}_0^{(1)}]^H\mathbf{n}_0. \tag{14}$$

Since the spatial feature of the steered interference is orthogonal to that of $\mathbf{u}_0^{(1)}$, the interfering terms can be canceled. So, the SE of PUE with MTIS can be computed as:

$$R_0 = \log_2\left\{1 + \frac{[\tilde{P}_{T_0} - \sum_{k=1}^{K}\tilde{P}_{MTIS}^{(k)}]\|[\mathbf{f}_0^{(1)}]^H\mathbf{H}_0\mathbf{p}_0^{(1)}\|^2}{\sigma_n^2}\right\}. \tag{15}$$

B. Design of Single-Target IS

Note that MTIS uses as many as $N_{R_0} - M$ DoFs to place the steered interference. If only one of $N_{R_0} - M$ DoFs is allowed for IM, MTIS becomes unavailable. In such a case, we design STIS to steer all the interference to an identical direction which incurs the cost of one DoF at the PUE. The K data streams sent from MBS require K steering signals each of which can adjust an interference to the same direction. Since we assume $N_{T_i} = N_{R_i} > 2$ $(i = 0, 1)$ and $M = 1$, the principal eigenmode with the largest channel gain is used for $x_0^{(1)}$'s transmission, then all the interference are steered to a direction lies in the subspace determined by the remaining $N_{R_0} - 1$ secondary eigenmodes. So, the received signal at PUE with STIS can be expressed as:

$$\mathbf{y}_0 = \sqrt{\tilde{P}_{T_0} - \sum_{k=1}^{K}\tilde{P}_{STIS}^{(k)}}\mathbf{H}_0\mathbf{p}_0^{(1)}x_0^{(1)} + \sum_{k=1}^{K}[\mathbf{t}^{(k)} + \mathbf{s}_{t,STIS}^{(k)}] + \mathbf{n}_0 \tag{16}$$

where $\tilde{P}_{STIS}^{(k)} = P_{STIS}^{(k)}10^{-0.1L_0}$ and $\mathbf{t}^{(k)} + \mathbf{s}_{t,STIS}^{(k)} = \sqrt{\frac{\tilde{P}_{T_1}}{K}}\mathbf{H}_{10}\mathbf{p}_1^{(k)}x_1^{(k)} + \sqrt{\tilde{P}_{STIS}^{(k)}}\mathbf{H}_0\mathbf{p}_{STIS}^{(k)}x_1^{(k)}$. $P_{STIS}^{(k)}$ and $\mathbf{p}_{STIS}^{(k)}$ represent the power overhead and the precoder of the steering signal for interference $\mathbf{t}^{(k)}$. With STIS, we first select an interference as the initial interference to which IS is applied, this interference along with the desired signal determines the direction to which the other $K-1$ interfering

signals are adjusted. In what follows, we adopt k^* where $k^* \in \{1, 2, \cdots, K\}$ as the index of the initial interference. We define

$$\mathbf{d}_{\mathbf{t}^{(k^*)}+\mathbf{s}_{t,STIS}^{(k^*)}} = \frac{\mathbf{t}^{(k^*)} + \mathbf{s}_{t,STIS}^{(k^*)}}{\|\mathbf{t}^{(k^*)} + \mathbf{s}_{t,STIS}^{(k^*)}\|}, \tag{17}$$

then $\mathbf{d}_{\mathbf{t}^{(k)}+\mathbf{s}_{t,STIS}^{(k)}} = \mathbf{d}_{\mathbf{t}^{(k^*)}+\mathbf{s}_{t,STIS}^{(k^*)}}$ where $k \in \{1, 2, \cdots, K\}\backslash\{k^*\}$, and $\langle \mathbf{d}_{\mathbf{s}}, \mathbf{d}_{\mathbf{t}^{(k^*)}+\mathbf{s}_{t,STIS}^{(k^*)}} \rangle = 0$ should hold. Recall that the spatial feature of the steering signal is determined by both the desired signal and the interference it is to adjust, we can first calculate $\mathbf{d}_{\mathbf{t}^{(k^*)}+\mathbf{s}_{t,STIS}^{(k^*)}} = \frac{\mathbf{t}_Q^{(k^*)}}{\|\mathbf{t}_Q^{(k^*)}\|}$ where $\mathbf{t}_Q^{(k^*)} = \mathbf{t}^{(k^*)} + \mathbf{s}_{t,STIS}^{(k^*)}$, and then compute the projection of the other interference $\mathbf{t}^{(k)}$ onto $\mathbf{d}_{\mathbf{t}^{(k^*)}+\mathbf{s}_{t,STIS}^{(k^*)}}$, i.e., $\mathbf{t}_Q^{(k)}$. Similarly to the analysis in the previous subsection, we can get $P_{STIS}^{(k^*)} = P_{MTIS}^{(k^*)}$ and $\mathbf{p}_{STIS}^{(k^*)} = \mathbf{p}_{MTIS}^{(k^*)}$. Since the interference indexed by k should be adjusted to the target direction $\mathbf{d}_{\mathbf{t}^{(k^*)}+\mathbf{s}_{t,STIS}^{(k^*)}}$, we can obtain

$$\mathbf{t}_Q^{(k)} = \sqrt{\frac{\tilde{P}_{T_1}}{K}} \mathbf{P}_{STIS} \mathbf{H}_{10} \mathbf{p}_1^{(k)} x_1^{(k)} \tag{18}$$

where

$$\mathbf{P}_{STIS} = \mathbf{d}_{\mathbf{t}^{(k^*)}+\mathbf{s}_{t,STIS}^{(k^*)}} [\mathbf{d}^H_{\mathbf{t}^{(k^*)}+\mathbf{s}_{t,STIS}^{(k^*)}} \mathbf{d}_{\mathbf{t}^{(k^*)}+\mathbf{s}_{t,STIS}^{(k^*)}}]^{-1} \times \mathbf{d}^H_{\mathbf{t}^{(k^*)}+\mathbf{s}_{t,STIS}^{(k^*)}} \tag{19}$$

is the projection matrix with respect to $\mathbf{d}_{\mathbf{t}^{(k^*)}+\mathbf{s}_{t,STIS}^{(k^*)}}$. By using $\mathbf{t}^{(k)} = \mathbf{t}_{In}^{(k)} + \mathbf{t}_Q^{(k)}$ and $\mathbf{s}_{t,STIS}^{(k)} = -\mathbf{t}_{In}^{(k)}$, we can get

$$\sqrt{\tilde{P}_{STIS}^{(k)}} \mathbf{H}_0 \mathbf{p}_{STIS}^{(k)} = -\sqrt{\frac{\tilde{P}_{T_1}}{K}} [\mathbf{H}_{10} \mathbf{p}_1^{(k)} - \mathbf{P}_{STIS} \mathbf{H}_{10} \mathbf{p}_1^{(k)}]. \tag{20}$$

Then, the implementation of STIS can be expressed as:

$$\begin{cases} \mathbf{p}_{STIS}^{(k^*)} = \mathbf{p}_{MTIS}^{(k^*)} \\ \mathbf{p}_{STIS}^{(k)} = -\dfrac{\mathbf{H}_0^{-1}[\mathbf{H}_{10}\mathbf{p}_1^{(k)} - \mathbf{P}_{STIS}\mathbf{H}_{10}\mathbf{p}_1^{(k)}]}{\|\mathbf{H}_0^{-1}[\mathbf{H}_{10}\mathbf{p}_1^{(k)} - \mathbf{P}_{STIS}\mathbf{H}_{10}\mathbf{p}_1^{(k)}]\|} \\ P_{STIS}^{(k^*)} = P_{MTIS}^{(k^*)} \\ P_{STIS}^{(k)} = \dfrac{P_{T_1}\varepsilon}{K} \|\mathbf{H}_0^{-1}[\mathbf{H}_{10}\mathbf{p}_1^{(k)} - \mathbf{P}_{STIS}\mathbf{H}_{10}\mathbf{p}_1^{(k)}]\|^2 \end{cases} \tag{21}$$

where $k^*, k \in \{1, 2, \cdots, K\}$ and $k \neq k^*$.

As illustrated in Fig. 2, the vectors in the figure indicate the spatial signals. Two interfering signals, $\mathbf{t}^{(1)}$ and $\mathbf{t}^{(2)}$ are involved. $\mathbf{t}_{In}^{(k)}$ where $k = 1, 2$ indicates the projection of interference $\mathbf{t}^{(k)}$ on the desired transmission, i.e., the in-phase component of interference with respect to the desired signal $\mathbf{s}$. $\mathbf{t}_Q^{(k)}$ denotes the quadrature component of interference with respect to $\mathbf{s}$. $\mathbf{s}_{t,STIS}^{(k)}$ is the steering signal for $\mathbf{t}^{(k)}$ with STIS. Given $K = 2$ interfering signals, we first determine the steering signal $\mathbf{s}_{t,STIS}^{(1)}$ for interference $\mathbf{t}^{(1)}$, i.e., $k^* = 1$, and then the steering signal for $\mathbf{t}^{(2)}$, i.e., $\mathbf{s}_{t,STIS}^{(2)}$, is computed. In practice, the initial interference may affect the performance of STIS. This will be discussed in the following subsection.

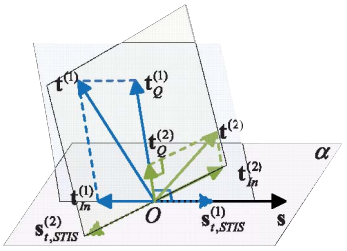

Fig. 2. An illustration of STIS under $K = 2$ and $N_{R_0} > 2$.

Similarly to the discussion of MTIS, when the interference is so strong that P_{T_0} is not sufficient for STIS, we simply switch to the non-IM mode. The expressions for the estimated signal at PUE by adopting $\mathbf{f}_0^{(1)} = \mathbf{u}_0^{(1)}$ as the receive filter and the SE of PUE with STIS can be obtained similarly to Eqs. (14) and (15). The only difference is that $\tilde{P}_{MTIS}^{(k)}$ should be replaced by $\tilde{P}_{STIS}^{(k)}$.

C. Analysis of Power Overhead for MTIS and STIS

We now analyze the power overheads of MTIS and STIS. Before delving into details, we first provide a theorem and a lemma necessary for this analysis.

Theorem 1: Minimum Angle Theorem – The angle between an oblique line passing through a plane and its projection on this plane is the minimum of all the angles between this oblique line and any line in the plane [26].

Lemma 1: The minimum power overhead for IS is achieved if and only if the desired signal, the original interference and the steered interference lie in the same plane.

See the proof of Lemma 1 in Appendix A.

With MTIS, an arbitrary interference $\mathbf{t}^{(k)}$ and its steered consequence $\mathbf{t}^{(k)} + \mathbf{s}_{t,MTIS}^{(k)}$ are in the same plane with the desired signal, and is thus power-cost optimal according to Theorem 1. On the other hand, for STIS, only the initial interference yields the minimum power cost (see in Fig. 2) while the other $K - 1$ do not. Therefore, the power overhead of STIS is larger than that of MTIS. Moreover, since the power cost of STIS is dependent on the selection of the initial interference, it can be minimized by optimally selecting an interference indexed by k^* according to:

$$k^* = \underset{k^* \in \{1,2,\cdots,K\}}{\arg\min} \left\{ P_{STIS}^{(k^*)} + \sum_{k=1, k\neq k^*}^{K} P_{STIS}^{(k)} \right\} \tag{22}$$

where $P_{STIS}^{(k^*)}$ and $P_{STIS}^{(k)}$ can be calculated by Eq. (21).

Note that MTIS's advantage over STIS in power cost is achieved on the premise that $N_{R_0} - M > 1$. If $N_{R_0} - M = 1$, MTIS steers all interference in one direction and incurs the same power overhead as STIS. That is, MTIS becomes STIS. In this sense, MTIS can subsume STIS as a special case.

IV. Design of Aggregated IS

Although MTIS and STIS can steer multiple interferences in the direction(s) orthogonal to the desired transmission, the steering signals will incur additional interference (regarded as

the side-effect of IS) to ongoing transmissions within their effective/coverage area. In addition, both methods achieve IM by steering interference individually. Since the essence of IM is limiting the influence of interference, i.e., the effective portion of interference imposed on the intended transmission, we can exploit the interactions, including constructive and destructive effect, among multiple interfering signals [27] in the design of IS. Here we propose an *aggregated interference steering* (AIS) by considering the overall effect of multiple interference. Similarly to Section III, our AIS design is based on one interfering MBS which sends $\mathbf{x}_1 = [x_1^{(1)} \ \cdots \ x_1^{(K)}]$, and with system setting $N_{T_i} = N_{R_i} > 2$ $(i = 0, 1)$. PBS employs BF to transmit to PUE. However, our design can be extended to more generalized cases (see in Section VI). In what follows, we will first elaborate on the design of AIS and then analyze its power overhead.

A. Signal Processing for AIS

The aggregated interference perceived by the interfered PUE is:

$$\mathbf{t}^{(\Sigma)} = \sum_{k=1}^{K} \sqrt{\frac{\tilde{P}_{T_1}}{K}} \mathbf{H}_{10} \mathbf{p}_1^{(k)} x_1^{(k)}. \tag{23}$$

Then, a steering signal can be generated to adjust $\mathbf{t}^{(\Sigma)}$ to the orthogonal direction with respect to the desired transmission. In order to exploit the interactions among the interference constituting $\mathbf{t}^{(\Sigma)}$, the inter-relationship of transmitted symbols carried by K interfering signals should be explored first. For clarity of exposition, we assume all the interfering signals employ the same modulation scheme. We use $S = \{s_1, s_2, \ldots, s_L\}$ to denote the symbol set. The size of S is $\text{card}(S) = L$ where $\text{card}(\cdot)$ represents the cardinality of set S, and L indicates the modulation order. Since each element in S can be represented by its amplitude and phase, we take an arbitrary symbol in S, say, s_i where $i \in \{1, 2, \ldots, L\}$, as an example, it can be expressed as $s_i = a_i e^{j\theta_i}$ where a_i and θ_i denote s_i's amplitude and phase, respectively. Let's define the transmitted symbol $x_1^{(\hat{k})} \in S$, i.e., $x_1^{(\hat{k})} = a_{\hat{i}} e^{j\theta_{\hat{i}}}$. Without loss of generality, we take $x_1^{(\hat{k})}$ as the referential symbol, then all the other symbols $x_1^{(k)}$ ($k \in \{1, 2, \ldots, K\}$ and $k \neq \hat{k}$) can be expressed in terms of $x_1^{(\hat{k})}$ as:

$$x_1^{(k)} = \frac{a_i}{a_{\hat{i}}} e^{j(\theta_i - \theta_{\hat{i}})} x_1^{(\hat{k})}. \tag{24}$$

Substituting Eq. (24) into Eq. (23) leads to Eq. (25), shown at the bottom of the next page, where $b_k = \frac{a_i}{a_{\hat{i}}} e^{j(\theta_i - \theta_{\hat{i}})}$ ($\hat{i}, i \in \{1, 2, \cdots, L\}$ and $\hat{i} \neq i$). $\mathbf{E} \in \mathbb{C}^{N_{R_0} \times 1}$ is the equivalent channel vector.

With AIS, by adopting $x_1^{(\hat{k})}$ as the referential symbol, the received signal at PUE is:

$$\begin{aligned} \mathbf{y}_0 = & \sqrt{\tilde{P}_{T_0} - \tilde{P}_{AIS}^{(\Sigma)}} \mathbf{H}_0 \mathbf{p}_0^{(1)} x_0^{(1)} \\ & + \sqrt{\frac{\tilde{P}_{T_1}}{K}} \mathbf{E} x_1^{(\hat{k})} + \sqrt{\tilde{P}_{AIS}^{(\Sigma)}} \mathbf{H}_0 \mathbf{p}_{AIS}^{(\Sigma)} x_1^{(\hat{k})} + \mathbf{n}_0 \end{aligned} \tag{26}$$

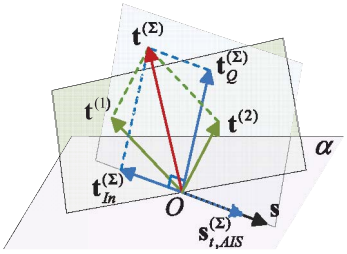

Fig. 3. An illustration of AIS under $K = 2$ and $N_{R_0} > 2$.

where $\tilde{P}_{AIS}^{(\Sigma)} = P_{AIS}^{(\Sigma)} 10^{-0.1L_0}$, $\tilde{P}_{AIS}^{(\Sigma)}$ and $\mathbf{p}_{AIS}^{(\Sigma)}$ denote the power overhead and the precoder of the steering signal for adjusting the aggregated interference $\sqrt{\frac{\tilde{P}_{T_1}}{K}} \mathbf{E} x_1^{(\hat{k})}$. Similar to the previous design, AIS can be realized according to Eq. (27) as:

$$\begin{cases} \mathbf{p}_{AIS}^{(\Sigma)} = -\dfrac{\mathbf{H}_0^{-1} \mathbf{P}_{AIS} \mathbf{E}}{\|\mathbf{H}_0^{-1} \mathbf{P}_{AIS} \mathbf{E}\|} \\ P_{AIS}^{(\Sigma)} = \dfrac{P_{T_1} \varepsilon}{K} \|\mathbf{H}_0^{-1} \mathbf{P}_{AIS} \mathbf{E}\|^2 \end{cases} \tag{27}$$

Fig. 3 illustrates the basic principle of AIS with $K = 2$, where we first obtain the aggregation of $\mathbf{t}^{(1)}$ and $\mathbf{t}^{(2)}$, denoted by $\mathbf{t}^{(\Sigma)}$, and then employ a steering signal $\mathbf{s}_{t,AIS}^{(\Sigma)}$ by using Eq. (27) to adjust $\mathbf{t}^{(\Sigma)}$'s spatial feature to the direction $\mathbf{d}_{\mathbf{t}^{(\Sigma)} + \mathbf{s}_{t,AIS}^{(\Sigma)}} = \frac{\mathbf{t}_Q^{(\Sigma)}}{\|\mathbf{t}_Q^{(\Sigma)}\|}$ which is orthogonal to the desired signal $\mathbf{s}$, where

$$\mathbf{d}_{\mathbf{t}^{(\Sigma)} + \mathbf{s}_{t,AIS}^{(\Sigma)}} = \frac{\sqrt{\frac{\tilde{P}_{T_1}}{K}} \mathbf{E} + \sqrt{\tilde{P}_{AIS}^{(\Sigma)}} \mathbf{H}_0 \mathbf{p}_{AIS}^{(\Sigma)}}{\left\| \sqrt{\frac{\tilde{P}_{T_1}}{K}} \mathbf{E} + \sqrt{\tilde{P}_{AIS}^{(\Sigma)}} \mathbf{H}_0 \mathbf{p}_{AIS}^{(\Sigma)} \right\|} \tag{28}$$

is the direction of $\mathbf{t}^{(\Sigma)}$ combined with the steering signal,

$$\mathbf{s}_{t,AIS}^{(\Sigma)} = \sqrt{\tilde{P}_{AIS}^{(\Sigma)}} \mathbf{H}_0 \mathbf{p}_{AIS}^{(\Sigma)} x_1^{(\hat{k})}. \tag{29}$$

$\mathbf{t}_{In}^{(\Sigma)}$ and $\mathbf{t}_Q^{(\Sigma)}$ denote the in-phase and quadrature components of $\mathbf{t}^{(\Sigma)}$ with respect to the desired signal.

When adopting $\mathbf{f}_0^{(1)} = \mathbf{u}_0^{(1)}$ as the receive filter, the estimated signal at PUE and the SE of PUE can be referred to Eqs. (14) and (15). The only difference is that $\sum_{k=1}^{K} \tilde{P}_{MTIS}^{(k)}$ should be replaced by $\tilde{P}_{AIS}^{(\Sigma)}$.

B. Analysis of Power Overhead for AIS

Here we analyze the power cost of AIS. Before delving into details, we first provide a theorem and a corollary necessary for this analysis.

Theorem 2: The projection of the aggregated interference on the desired signal is equal to the sum of all of the interfering signals' projections onto the desired transmission.

See the proof of Theorem 2 in Appendix B.

Corollary 1: When multiple interfering signals strengthen (weaken) each other, the power overhead of AIS is larger (less) than that of MTIS.

See the proof of Corollary 1 in Appendix C.

Fig. 4 illustrates the various types of interactions among two interfering signals, where $\mathbf{t}^{(k)}$ $(k = 1, 2)$ and $\mathbf{t}^{(\Sigma)}$ lie

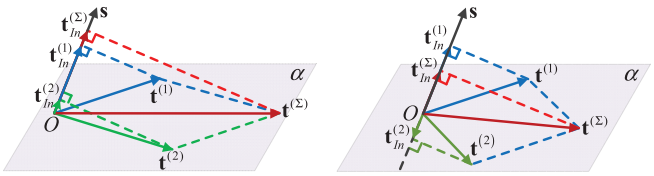

(a) Constructive situation. (b) Destructive situation.

Fig. 4. Various types of interactions among $K = 2$ interfering signals. (a) Constructive situation. (b) Destructive situation.

in plane α, whereas $\mathbf{s}$, $\mathbf{t}_{In}^{(\Sigma)}$ and $\mathbf{t}_{In}^{(k)}$ do not. As shown in Fig. 4(a), when the spatial features of the two interference are positively correlated, we can get $\rho_{12} > 0$ where ρ_{12} denotes the correlation between two disturbances indexed by 1 and 2 (see in Appendix C). Then, we have $P_{AIS}^{(\Sigma)} > \sum_{k=1}^{2} P_{MTIS}^{(k)}$; whereas in Fig. 4(b), the two interfering signals are negatively correlated, incurring $\rho_{12} < 0$, thus resulting in $P_{AIS}^{(\Sigma)} < \sum_{k=1}^{2} P_{MTIS}^{(k)}$.

According to Eqs. (46) and (48) in Appendix C, AIS's power cost is obtained as $P_{AIS}^{(\Sigma)} = \sum_{k=1}^{K} P_{MTIS}^{(k)} + 2 \cdot 10^{0.1L_0}\rho_\Sigma$ where $\rho_\Sigma = \sum_{k=1}^{K-1}\sum_{k'=k+1}^{K}\rho_{kk'}$ and $\rho_{kk'} = \mathrm{Re}\{[\mathbf{H}_0^{-1}\mathbf{t}_{In}^{(k)}]^H[\mathbf{H}_0^{-1}\mathbf{t}_{In}^{(k')}]\}$. $\rho_{kk'}$ indicates the correlation between two disturbances indexed by k and k', $k, k' \in \{1, 2, \cdots, K\}$ and $k \neq k'$. Based on the discussion in Section III-C, we can have $\sum_{k=1}^{K} P_{MTIS}^{(k)} < \sum_{k=1}^{K} P_{STIS}^{(k)}$ on premise that $N_{R_0} - M > 1$. Thus, provided with $N_{R_0} - M > 1$, when $\rho_\Sigma < 0$, we can obtain $P_{AIS}^{(\Sigma)} < \sum_{k=1}^{K} P_{MTIS}^{(k)} < \sum_{k=1}^{K} P_{STIS}^{(k)}$. Otherwise, when $\rho_\Sigma > 0$, $\sum_{k=1}^{K} P_{MTIS}^{(k)}$ yields the least power cost. In addition, given $N_{R_0} - M = 1$, MTIS becomes STIS. So, in the following discussion, we only focus on the adaptation of MTIS and AIS in terms of their power-efficiency.

Based on the above discussion, the adaptation between MTIS and AIS can be achieved based on the characteristic of ρ_Σ:

$$\begin{cases} \text{Adopt MTIS}, & \text{when } \rho_\Sigma > 0 \\ \text{Adopt AIS}, & \text{when } \rho_\Sigma < 0 \end{cases} \tag{30}$$

So far, we have proved that the power cost of MTIS is less than that of STIS (see in Section III-C). STIS and AIS incur only one DoF cost at the interfered receiver. In summary, STIS reduces the DoF cost at the expense of more power overhead, whereas MTIS saves interfered transmitter's power at the cost of more DoF consumption. As compared to the two IIS schemes, AIS is shown to be advantageous in both power cost and DoF consumption.

V. Generalization of Different IS Mechanisms

A. Generalized Number of PBSs and PUEs

So far, we have assumed that one MBS sends multiple data streams to a MUE, and considered only one interfered transmission pair. When multiple PBSs are deployed in the coverage of a macrocell and multiple PUEs are served by each PBS, the proposed schemes can be extended [21].

B. Generalized Number of MBSs and MUEs

We now generalize the number of MBSs deployed in the communication system and the number of MUEs served by each MBS. Since pico-cells are always deployed within the coverage of one MBS, the disturbance(s) from this MBS dominates the other MBSs. Thus, we do not consider the interference from those adjacent MBSs in our current design. However, since the proposed three IS schemes are the interfered transmitter centric, i.e., the interfered PBS carries out MTIS, STIS or AIS, the processing in multi-MBS case considering interference from adjacent MBSs is the same as that in the case of one MBS discussed so far, thus making our methods directly applicable. The only difference is that the interference information required by the interfered PBS is from multiple interfering MBSs. In the multi-MUE situation, the proposed IS realizations can also be directly applied due to their interfered Tx centric feature. In other words, the application of our methods is independent of the transmission mode of interferer(s).

In the above multi-MBS discussion, we simply assume all interfering MBSs are coordinated, i.e., the status of disturbances from the MBSs can be obtained by PBS for generation of steering signal(s). However, it is not necessary in practice to coordinate all MBSs, and hence the uncoordinated interference from MBSs that do not belong to the coordination cluster can constitute a major factor in the performance of cellular systems [28]–[30]. [28], [29] of these modeled both intra-cluster interference (ICI) and out-of-the-coordination-cluster interference (OCI), and considered them in the evaluation of CoMP transmission performance. The authors of [30] proposed novel optimized transceivers for multiuser multi-cell networks in both the uplink and the downlink by minimizing

$$\begin{aligned}
\mathbf{t}^{(\Sigma)} &= \sqrt{\frac{\tilde{P}_{T_1}}{K}}\mathbf{H}_{10}\mathbf{p}_1^{(\hat{k})}x_1^{(\hat{k})} + \sum_{k=1,k\neq\hat{k}}^{K}\sqrt{\frac{\tilde{P}_{T_1}}{K}}\mathbf{H}_{10}\mathbf{p}_1^{(k)}x_1^{(k)} \\
&= \sqrt{\frac{\tilde{P}_{T_1}}{K}}\mathbf{H}_{10}\mathbf{p}_1^{(\hat{k})}x_1^{(\hat{k})} + \sum_{k=1,k\neq\hat{k}}^{K}\sqrt{\frac{\tilde{P}_{T_1}}{K}}\mathbf{H}_{10}\mathbf{p}_1^{(k)}\left[\frac{a_i}{a_{\hat{i}}}e^{j(\theta_i-\theta_{\hat{i}})}x_1^{(\hat{k})}\right] \\
&= \sqrt{\frac{\tilde{P}_{T_1}}{K}}\left[\mathbf{H}_{10}\mathbf{p}_1^{(\hat{k})} + \sum_{k=1,k\neq\hat{k}}^{K}\mathbf{H}_{10}\mathbf{p}_1^{(k)}b_k\right]x_1^{(\hat{k})} = \sqrt{\frac{\tilde{P}_{T_1}}{K}}\mathbf{E}x_1^{(\hat{k})}
\end{aligned} \tag{25}$$

the total mean-square error (MSE) at each base station given that out-of-cell precoders and the cross-channel information for weaker interferers are not known. Moreover, it was shown in [31] that although coordination is viewed as a key ingredient for IM in wireless networks, there is a fundamental limitation of cooperation. Specifically, for a cellular system, as a result of OCI, the spectral efficiency (SE) inevitably gets saturated for increasing transmit power at each transmitter whenever a system is arranged into cooperation clusters. Hence, we will evaluate the performance of the proposed schemes with uncoordinated interference in Section VI.

C. Generalized Number of Desired Data Streams

We now generalize the number, M, of desired signals sent from one interfered PBS to its PUE [21]. The data vectors from PBS and the interfering MBS are denoted by $\mathbf{x}_0 = [x_0^{(1)}\ x_0^{(2)}\ \cdots\ x_0^{(M)}]^T$ and $\mathbf{x}_1 = [x_1^{(1)}\ x_1^{(2)}\ \cdots\ x_1^{(K)}]^T$, respectively. With MTIS, we let $N_{R_0} > M+1$. Since M desired data streams are sent from PBS to PUE via mutually orthogonal eigenmodes/subchannels, the interference can be either individually (IIS) or aggregately (regarded as AIS) steered to the remaining unoccupied eigenmode(s)/subchannel(s). By referring to Sections III and IV, the general expressions of the received and estimated signal at PUE, and the SE of PUE are given as:

$$\mathbf{y}_0 = \sum_{m=1}^{M} \sqrt{\frac{\tilde{P}_{T_0} - \tilde{\mathcal{P}}_{\mathcal{M}}}{M}} \mathbf{H}_0 \mathbf{p}_0^{(m)} x_0^{(m)} + \sqrt{\frac{\tilde{P}_{T_1}}{K}} \sum_{k=1}^{K} \mathbf{H}_{10} \mathbf{p}_1^{(k)} x_1^{(k)} + \mathcal{S}_{t,\mathcal{M}} + \mathbf{n}_0 \tag{31}$$

$$\bar{y}_0 = \sum_{m=1}^{M} \sqrt{\frac{\tilde{P}_{T_0} - \tilde{\mathcal{P}}_{\mathcal{M}}}{M}} \mathbf{F}^H \mathbf{H}_0 \mathbf{p}_0^{(m)} x_0^{(m)} + \mathbf{F}^H \mathbf{n}_0 \tag{32}$$

$$R_0 = \sum_{m=1}^{M} \log_2 \left\{ 1 + \frac{(\tilde{P}_{T_0} - \tilde{\mathcal{P}}_{\mathcal{M}}) \| [\mathbf{f}_0^{(m)}]^H \mathbf{H}_0 \mathbf{p}_0^{(m)} \|^2}{M \sigma_n^2} \right\} \tag{33}$$

where $x_0^{(m)}$ $(m = 1, 2, \ldots, M)$ denotes the m^{th} data stream sent from PBS, and $\mathbf{p}_0^{(m)}$ is the precoder for $x_0^{(m)}$. We employ $\mathbf{F} = [\mathbf{f}_0^{(1)}\ \cdots\ \mathbf{f}_0^{(m)}\ \cdots\ \mathbf{f}_0^{(M)}]^T$ as the receive filter at PUE to decode M data streams. Scalar $\mathcal{P}_{\mathcal{M}}$ represents for the power overhead of various IS implementations. $\tilde{\mathcal{P}}_{\mathcal{M}} = \mathcal{P}_{\mathcal{M}} 10^{-0.1 L_0}$. The subscript $\mathcal{M} \in \{\text{MTIS}, \text{STIS}, \text{AIS}\}$ indicates the IS scheme we employed. $\mathcal{S}_{t,\mathcal{M}}$ denotes either the sum of K steering signals with IIS or one steering signal with AIS. We apply SVD to $\mathbf{H}_0$ to obtain $\mathbf{H}_0 = \mathbf{U}_0 \mathbf{\Sigma}_0 \mathbf{V}_0^H$ and employ $\mathbf{p}_0^{(m)} = \mathbf{v}_0^{(m)}$ and $\mathbf{f}_0^{(m)} = \mathbf{u}_0^{(m)}$. Then, the IS schemes proposed in Sections III and IV can be directly applied.

D. Generalized CSI and Channel Model Assumptions

So far, we have presented various IS implementations under instantaneous and perfect CSI, which is difficult to be obtained in practice, especially for fast varying channels. Therefore, exploiting statistical CSI (S-CSI) instead of instantaneous CSI (I-CSI) would be easier and cost-effective. Although S-CSI is somewhat more realistic than I-CSI, its inaccuracy may incur some performance loss compared to the schemes based on I-CSI [32]. Moreover, the I-CSI-based designs and the results therein could still provide some theoretical conclusions. The extension of our schemes to the case of using S-CSI can be found in [17], [18], [32]. Since the design of IS schemes under S-CSI is beyond our scope, it is not elaborated in this paper.

There are several causes of partial CSI (or CSI error), including estimation error, CSI quantization, etc. The improvement of system performance is shown to be susceptible to the accuracy of CSI [33], [34]. The channel matrix can be modeled to account for CSI error as [33]–[35]:

$$\widehat{\mathbf{H}} = \rho \mathbf{H} + \sqrt{1 - \rho^2} \mathbf{\Xi} \tag{34}$$

where $\mathbf{H}$ and $\widehat{\mathbf{H}}$ denote accurate and inaccurate channel matrices, respectively. Coefficient $\rho \in (0, 1]$ indicates the degree of CSI imperfection and $\rho = 1$ means perfect CSI. Matrix $\mathbf{\Xi}$ is an $N_R \times N_T$ diagonal complex Gaussian matrix with zero mean and unit variance where N_R and N_T are the numbers of antennas equipped with the receiver and transmitter of a MIMO link. As shown in [36], [37], ρ can be used to indicate the impact of several factors on CSI, and hence is a function of the length of training sequence, signal-to-noise ratio (SNR) and Doppler frequency shift.

To improve the robustness of the proposed IS to imperfect CSI, one can devise an iterative method based on either minimum mean-square error (MMSE) [29], [38], [39] or maximum signal-to-interference-plus-noise ratio (SINR) [29], [40]. By exploiting the reciprocity/duality of wireless networks, a Max-SINR algorithm was proposed in [40] to obtain receive filters and precoding vectors so as to maximize SINR at the Rxs. Our IS implementations are likewise modified by first applying MTIS/STIS/AIS to multiple disturbances, and then employing the Max-SINR algorithm to iteratively adjust the precoder and the receive filter at the transmitter and receiver of the interfered transmission pair, so that the interfered Rx's reception can be enhanced. Our schemes as well as their improvements under imperfect CSI will be evaluated in Section VI.

Here we employ a spatially uncorrelated MIMO channel for simplicity. However, a spatially correlated channel, $\mathbf{H} = \mathbf{R}_r^{1/2} \mathbf{H}_{iid} \mathbf{R}_t^{1/2}$, may be suitable [41], where $\mathbf{H}_{iid}$ is the spatially uncorrelated channel matrix, $\mathbf{R}_t$ and $\mathbf{R}_r$ represent the spatial complex correlation matrices at the Tx and the Rx, respectively. The coefficients in $\mathbf{R}_t$ and $\mathbf{R}_r$ depend on such physical parameters as antenna spacing, antenna arrangement, angle spread, and angle of arrival [42]. Therefore, given a spatially correlated channel, our proposed schemes can be applied. What we need is the calculation of $\mathbf{R}_t$ and $\mathbf{R}_r$ based on the system settings, and then use $\mathbf{H}$ instead of $\mathbf{H}_{iid}$ for the calculation of steering signal(s). Since the focus of the statistical CSI could be a problem in its own right, we would consider it in our future work.

VI. Analysis of Computational Complexity

We now analyze the computational complexity of the proposed schemes. The complexities are quantified in number of

TABLE I
THE COMPLEXITY OF MAIN OPERATIONS

$\mathbf{A}_1 + \mathbf{A}_1$	$2mn$
$\mathbf{A}_1\mathbf{A}_2$	$6mnp + 2mp(n-1)$
$\mathbf{A}_3^{-1}$	$6m^3 + 2m(m-1)^2$
Normalization($\mathbf{A}_1$)	$10mn$
SVD($\mathbf{A}_1$)	$24m^2n + 48mn^2 + 54n^3$ [44]

TABLE II
THE COMPLEXITY OF VARIOUS IM METHODS

Method	Complexity
MTIS	$\sim 8N_R^3 + 72N_R^2N_T + 104N_RN_T^2 + 108N_T^3 + 8KN_T^2$
STIS	$\sim 16N_R^3 + 96N_R^2N_T + 112N_RN_T^2 + 108N_T^3 + 8KN_T^2$
AIS	$\sim 8N_R^3 + 72N_R^2N_T + 96N_RN_T^2 + 108N_T^3 + 8KN_RN_T$
IN	$\sim 8N_R^3 + 72N_R^2N_T + 96N_RN_T^2 + 108N_T^3 + 8KN_T^2$
ZF	$\sim 48N_R^2N_T + 96N_RN_T^2 + 108N_T^3 + 8K^3 + 16K^2N_R$

real floating-point operations (FLOPs) [43]. A real addition, multiplication, or division is counted as one FLOP. A complex addition and multiplication have two FLOPs and six FLOPs, respectively. For clarity of exposition, we consider system settings of 2-transmitter 2-receiver with variable N_T and N_R, single desired/interfered transmission and K interference. All of the following operations are assumed in complex domain calculations. The complexity of main operations related to the proposed schemes is given in Table I, where $\mathbf{A}_1 \in \mathbb{C}^{m\times n}$, $\mathbf{A}_2 \in \mathbb{C}^{n\times p}$ and $\mathbf{A}_3 \in \mathbb{C}^{m\times m}$. SVD($\mathbf{A}_1$) and Normalization($\mathbf{A}_1$) indicate application of SVD and computation of the normalization of $\mathbf{A}_1$, respectively. The symbol "$\sim$" represents an asymptotic value as as $m, n, p \to \infty$ (leading terms). In what follows, the computational complexity at transmitter and receiver sides will be detailed.

We first analyze the complexity of MTIS at PBS and PUE, respectively, under $1 < K \leq N_R - 1$ interference. According to Eq. (13), we need to calculate $\mathbf{p}_{MTIS}^{(k)}$ and $P_{MTIS}^{(k)}$, where $k \in \{1, \ldots, K\}$. To obtain $\mathbf{p}_{MTIS}^{(k)}$, we first need to apply SVD to $\mathbf{H}_0$, which takes $24N_R^2N_T + 48N_RN_T^2 + 54N_T^3$ FLOPs. As for a matrix $\mathbf{H} \in \mathbb{C}^{N_R\times N_T}$, when $N_T > N_R$, according to the Moore-Penrose pseudo-inverse calculation $\mathbf{H}^\dagger = \mathbf{H}^H(\mathbf{H}\mathbf{H}^H)^{-1}$, two matrix multiplications and one matrix inversion are needed, so the total FLOP count is $8N_R^3 + 16N_R^2N_T - 6N_R^2 - 2N_RN_T + 2N_R$ in total. Without loss of generality, we first analyze the complexity of applying MTIS to the interference indexed by 1. To compute $\mathbf{p}_{MTIS}^{(1)}$, we need to calculate $\mathbf{P}_{MTIS} = \mathbf{d_s}\mathbf{d_s}^H = \frac{\mathbf{H}_0\mathbf{p}_0^{(1)}}{||\mathbf{H}_0\mathbf{p}_0^{(1)}||}\left[\frac{\mathbf{H}_0\mathbf{p}_0^{(1)}}{||\mathbf{H}_0\mathbf{p}_0^{(1)}||}\right]^H$, which requires multiplication of an $N_R \times N_T$ matrix and an $N_T \times 1$ vector, normalization of $N_R \times 1$ vector, and multiplication of an $N_R \times 1$ vector and a $1 \times N_R$ vector. Then, the FLOP count of $\mathbf{P}_{MTIS}$ is $6N_R^2 + 8N_RN_T + 8N_R$. To get $\mathbf{H}_0^{-1}\mathbf{P}_{MTIS}\mathbf{H}_{10}$, multiplication of an $N_T \times N_R$ matrix and an $N_R \times N_R$ matrix and multiplication of an $N_T \times N_R$ matrix and an $N_R \times N_T$ matrix are needed, so the FLOP count is $8N_R^2N_T + 8N_RN_T^2 - 2N_RN_T - 2N_T$. Therefore, according to the first equation of Eq. (13), to obtain $\mathbf{p}_{MTIS}^{(1)}$, a multiplication of an $N_T \times N_T$ matrix and an $N_T \times 1$ vector and a normalization of $N_T \times 1$ vector are required, so the FLOP count is $8N_T^2 + 8N_T$. To get $P_{MTIS}^{(1)}$, multiplication of a $1 \times N_T$ vector and an $N_T \times 1$ vector (to obtain $||\mathbf{H}_0^{-1}\mathbf{P}_{MTIS}\mathbf{H}_{10}\mathbf{p}_1^{(1)}||^2$ in the second equation of Eq. (13)) and three real multiplications are needed, so the FLOP count is $8N_T + 1$. Since $\mathbf{P}_{MTIS}$ of all interference is the same, $\mathbf{P}_{MTIS}$ and $\mathbf{H}_0^{-1}\mathbf{P}_{MTIS}\mathbf{H}_{10}$ are computed only once. Then, to get $\mathbf{p}_{MTIS}^{(k)}$ and $P_{MTIS}^{(k)}$ for the rest $K-1$ disturbances, $8KN_T^2 + 16KN_T - 32N_T - K - 16N_T^2 + 2$ FLOPs are needed. As a result, the FLOP count of MTIS with K disturbances at the PBS side is $8N_R^3 + 48N_R^2N_T + 56N_RN_T^2 + 54N_T^3 + 4N_RN_T + 8KN_T^2 - 2N_T^2 + 10N_R - K + 16KN_T + 2$.

At the PUE side, we first need to apply SVD to $\mathbf{H}_0$, which takes $24N_R^2N_T + 48N_RN_T^2 + 54N_T^3$ FLOPs. Then, according to Eq. (14), multiplication of a $1 \times N_R$ filter vector and an $N_R \times 1$ received signal vector is needed, so the FLOP count is $8N_R - 2$. Therefore, the total FLOP count at PUE is $24N_R^2N_T + 48N_RN_T^2 + 54N_T^3 + 8N_R - 2$.

Based on the above analysis, the total FLOP count for realizing MTIS is $8N_R^3 + 72N_R^2N_T + 104N_RN_T^2 + 108N_T^3 + 4N_RN_T + 8KN_T^2 - 2N_T^2 + 18N_R + 16KN_T - K$.

Similarly, we can compute the complexities of STIS and AIS. Compared to MTIS, the realization of STIS requires two times calculation (the second time calculation can be referred to Eq. (19)) of the projection matrix, then its complexity is $16N_R^3 + 96N_R^2N_T + 112N_RN_T^2 + 108N_T^3 + 2N_RN_T + 8KN_T^2 - 4N_T^2 + 32N_R + 16KN_T - K$ FLOPs. As for AIS, it first adds K disturbances to obtain the aggregated interference, then one steering signal is generated accordingly. Since $\mathbf{p}_{AIS}^{(\sum)}$ and $P_{AIS}^{(\sum)}$ are computed only once, the complexity of AIS is $8N_R^3 + 72N_R^2N_T + 96N_RN_T^2 + 108N_T^3 + 12N_RN_T + 8KN_RN_T + 24N_R + 16N_T + 4KN_R + 8K - 9$ FLOPs in total.

As a comparison, the complexities of IN and ZF are analyzed as follows. With IN, there is no need to compute the projection matrix, reducing computational burden at the interfered transmitter side. As for ZF reception, the complexity is mainly due to the SVD of $\mathbf{H}_0$ and the calculation of filter matrix $\mathbf{W}_{ZF} = (\overline{\mathbf{H}}^H\overline{\mathbf{H}})^{-1}\overline{\mathbf{H}}^H$ at the receiver side where $\overline{\mathbf{H}} = [\mathbf{h}_0 \ \cdots \ \mathbf{h}_k \ \cdots \ \mathbf{h}_K]$, $\mathbf{h}_0 = \mathbf{H}_0\mathbf{p}_0^{(1)}$ and $\mathbf{h}_k = \mathbf{H}_{10}\mathbf{p}_1^{(k)}$ $(1 \leq k \leq K)$.

Based on the above analysis, we summarize the complexity of the above IM schemes in Table II.

The above analysis is under the assumption of $N_T > N_R$. When $N_T = N_R$, the pseudo-inverse of a matrix should be replaced by its inverse. The Gauss-Jordan elimination can be employed to compute the inverse of an $N_R \times N_R$ matrix, which takes $6N_R^3 + 2N_R(N_R-1)^2$ FLOPs. As for the remaining computations, they are the same as those in the $N_T > N_R$ situation. So, we omit the detailed analysis.

VII. NUMERICAL STUDIES

We evaluate the performance of the proposed three IS implementations using MATLAB simulation. We set $d = 300$m, $D = 3000$m, $P_{T_0} = 23$dBm and $P_{T_1} = 46$dBm [23]. The path loss [23] is set to $L_{10} = 128.1 + 37.6\log_{10}(\eta_{10}/10^3)$ dB and $L_0 = 38 + 30\log_{10}\eta_0$ dB where $\eta_{10} \leq D$ and $\eta_0 \leq d$, respectively. In practice, PUE may be indoor, and our path loss model of L_0 has taken the wall loss into account [23]. As for

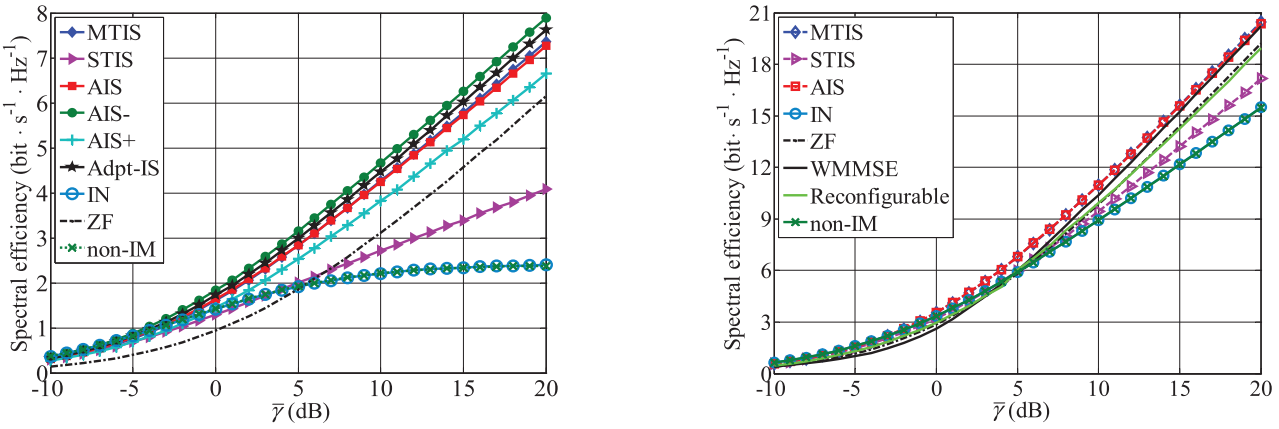

(a) PUE's SE. (b) System's SE.

Fig. 5. SE vs. $\bar{\gamma}$ under $\xi = 0.5$ and $N_{T_0} = N_{R_0} = N_{T_1} = 3$. (a) PUE's SE. (b) System's SE.

the other typical type of fading (i.e., shadow fading), since it can be characterized by log normal fading with 10dB and 6dB standard deviations in macro and pico cells, respectively [23], the path loss models with shadow fading only need to add constant deviations to those without shadow fading. That is, we do not explicitly discuss wall loss or shadow fading, but the results and conclusions in this paper can be extended to the case of above-mentioned loss/fading. Since L_0 and L_{10} are dependent on the network topology, $\tilde{P}_{T_0}$ ranges from -89dBm to 23dBm, whereas $\tilde{P}_{T_1}$ varies between -100dBm to 46dBm. For clarity of presentation, we adopt $\bar{\gamma} = 10\log_{10}\gamma$ where $\gamma = \tilde{P}_{T_0}/\sigma_n^2$. We also define $\xi = \tilde{P}_{T_0}/\tilde{P}_{T_1}$. Then, based on these parameter settings, we can get $\xi \in [-135, 123]$dB. Note, however, that since we obtained this result for extreme boundary situations, its range is too wide to be useful. In practice, a PBS should not be deployed close to MBS and mobile users may select an access point based on the strength of reference signals from multiple access points. Considering this practice, we set $\xi \in [0.1, 100]$ in our simulation. When P_{T_0} is not sufficient for implementing IS, non-IM is adopted. With non-IM, the interfered Rx employs MF to decode its desired data while leaving the interference un-managed. This is similar to the case of uncoordinated interference where the status of interference cannot be obtained for IM. Therefore, non-IM can be employed as a base line in the evaluation of the proposed IS-based schemes. There are M desired signals and K disturbances. Without specifications, the simulation is under $M = 1$ desired signals and $K = 2$ interference. Moreover, the evaluation of all schemes is under an identical power constraint. That is, the transmit power is divided into two parts: the one for generating the steering signal and the other for the desired signal's transmission.

Besides the proposed schemes, several IM methods based on interfered-transmission-pairs including ZF, IN, IS [15], WMMSE (Weighted Minimum Mean-Square Error) [38] and the reconfigurable algorithm [39] are also simulated for comparison. Since MTIS can be regarded as the extension of IS to the multi-interference case, the performance of IS can be referred to that of MTIS. WMMSE is a linear transceiver design algorithm for the MIMO interfering broadcast channel (IBC) where multiple base stations in a cellular network simultaneously transmit signals to a group of users in their own cells while causing interference to each other [38]. Via iterative minimization of weighted MSE, WMMSE can maximize the system's weighted sum-rate. The reconfigurable algorithm [39], designed for K-user MIMO interference channel (IFC), can automatically adjust itself to the interference levels and the wireless channel conditions, and by combining the system-wide MMSE criterion with the single-user water-filling solution, each user's transmission rate is maximized.

Fig. 5 shows the average SE (computed by using Monte-Carlo simulation) of different IS implementations under $\xi = 0.5$ and $N_{T_0} = N_{R_0} = N_{T_1} = 3$. In Fig. 5(a), PUE's SE is simulated. We also plot the average SE of PUE with AIS under $\rho_\Sigma < 0$ and $\rho_\Sigma > 0$, denoted by AIS$-$ and AIS$+$, respectively. When the two interfering signals are positively correlated ($\rho_\Sigma > 0$), the SE of AIS$+$ is shown to be inferior to that of AIS, whereas for the negatively correlated situation ($\rho_\Sigma < 0$) AIS$-$ outperforms AIS. Due to the randomness of wireless channels and transmitted symbols, both cases of $\rho_\Sigma > 0$ and $\rho_\Sigma < 0$ occur with approximately the same probability, and thus the SE of AIS lies between AIS$+$ and AIS$-$. Since the power overhead of STIS is higher than that of MTIS (see in Section III-C), STIS yields poorer SE than MTIS. The adaptation of AIS and MTIS, denoted by Adpt-IS, outperforms the other schemes. With IN, the power overhead for neutralizing interference grows with an increase of $\bar{\gamma}$, when the power cost exceeds the transmit power at PBS, MF is employed for reception, so that SE of IN gradually saturates as $\bar{\gamma}$ increases. Given $\xi = 0.5$, the power budget for IN at PBS is small relative to the strength of interference perceived by the PUE, so the probability of adopting MF is high, incurring SE of non-IM overlapping with that of IN [8]. It should be noted that both IN and IS implementations rely on $\mathbf{H}_0$, $\mathbf{H}_{10}$, and interfering data $\mathbf{x}_1$, so neither of them is applicable in the absence of inter-BS cooperation. However, since ZF reception is realized based on $\mathbf{H}_0$ and $\mathbf{H}_{10}$, it can be employed as a base line in terms of the degree of cooperation.

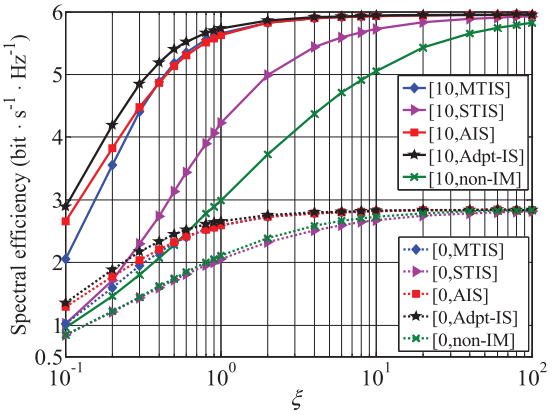

Fig. 6. SE of PUE vs. ξ under $N_{T_0} = N_{R_0} = N_{T_1} = 3$ and different $\bar{\gamma}$s.

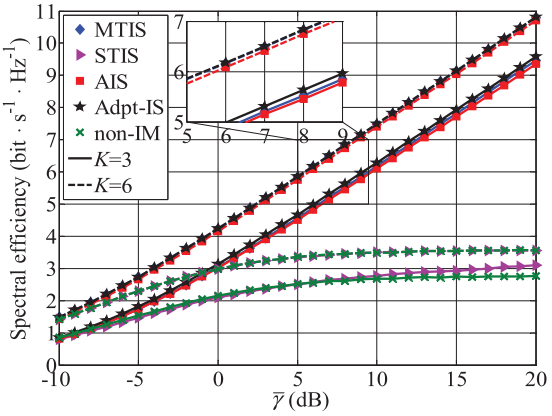

Fig. 7. SE of PUE vs. $\bar{\gamma}$ under $\xi = 0.5$, $M = 1$ and different Ks.

Since WMMSE [38] and the reconfigurable algorithm [39] are realized by iteratively adjusting the precoders and the receive filters at the interfering/interfered transmitter(s) and receiver(s), respectively, we plot in Fig. 5(b) the system's SE of various schemes. Note that like MTIS, all of STIS, AIS, IN and ZF are IM methods based on interfered-transmission-pair, and hence SE of the interfering user-pair is unaffected, i.e., a point-to-point MIMO transmission is realized under the multi-antenna system settings. Therefore, the interrelations of the SE performance of these methods are consistent with those in Fig. 5(a). As the figure shows, the proposed MTIS and AIS can yield slightly higher SE than WMMSE [38] and the reconfigurable algorithm [39]. However, our methods do not sacrifice the interfering transmissions as WMMSE and reconfigurable algorithm do.

It should be noted that when given $N_{T_0} = N_{R_0} = N_{T_1} = 2$, the number of signal components, i.e., desired signal and interference, exceeds N_{R_0}, and thus ZF is unavailable. In such a situation, SEs of MTIS and STIS will completely overlap with each other since when $N_{R_0} = 2$ only one DoF can be used to place interference. Therefore, MTIS becomes STIS (see in Section III-C), so both have the same average SE. Due to space limitation, we omit the simulation.

Fig. 6 shows the PUE's average SE along with ξ under $N_{T_0} = N_{R_0} = N_{T_1} = 3, \bar{\gamma} = 0$dB and $\bar{\gamma} = 10$dB, respectively. We use a general form $[\bar{\gamma}, \mathcal{M}]$ to denote the parameter settings, where $\mathcal{M}$ indicates the type of IS implementation. As shown in the figure, the PUE's SE improves as $\bar{\gamma}$ increases. From Eq. (33), we can also obtain

$$R_0 = \sum_{m=1}^{M} \log_2 \left\{ 1 + \frac{(\frac{1}{M} - \frac{\tilde{\mathcal{P}}_{\mathcal{M}}}{M\xi \tilde{P}_{T_1}}) \|[\mathbf{f}_0^{(m)}]^H \mathbf{H}_0 \mathbf{p}_0^{(m)}\|^2}{\frac{\sigma_n^2}{P_{T_0}}} \right\}, \tag{35}$$

so the average SE of PUE improves as ξ increases. However, as ξ gets too large, ξ^{-1} approaches 0, and thus the average SE of PUE gets saturated as ξ increases. Given fixed $\bar{\gamma}$, SE of non-IM grows as ξ increases since a relatively high transmit power is available at PBS.

As Fig. 6 shows, the difference between AIS's and MTIS's SE under small ξ is more pronounced than that under large ξ. This is analyzed as follows. According to the analysis provided in Section IV-B, when the spatial features of K disturbances are positively correlated, we can get $\rho_\Sigma > 0$ and $P_{AIS}^{(\Sigma)} > \sum_{k=1}^{K} P_{MTIS}^{(k)}$. When they are negatively correlated, we get $\rho_\Sigma < 0$ and $P_{AIS}^{(\Sigma)} < \sum_{k=1}^{K} P_{MTIS}^{(k)}$. Given $\rho_\Sigma < 0$, multiple interfering signals destroy each other, thus resulting in a weakened effective interference. When $\rho_\Sigma > 0$, multiple disturbances construct each other, yielding a strengthened equivalent interference at the interfered Rx.

Moreover, recall that given a small ξ, the strength of interference is relatively high compared to the desired signal. Then, under $\rho_\Sigma < 0$ and small ξ, PUE's SE with AIS is enhanced due to the reduced power cost whereas the feasible probability of MTIS decreases, compared to those under large ξ. Therefore, AIS outperforms MTIS in SE under a small ξ, and furthermore, the advantage of AIS over MTIS grows as ξ decreases. Given $\rho_\Sigma > 0$, AIS suffers severer SE degradation than MTIS when ξ is small due to the strengthened interference. Moreover, the feasible probability of both AIS and MTIS reduces as ξ decreases and becomes close to each other when ξ becomes extremely small. In addition, due to the randomness of channel status, $\rho_\Sigma < 0$ and $\rho_\Sigma > 0$ occur with the same probability. So, the smaller ξ, the larger the difference between AIS's and MTIS's SE.

Fig. 7 shows the PUE's average SE vs. $\bar{\gamma}$ under $\xi = 0.5$, $M = 1$ and different Ks. For MTIS, given K disturbances, we set $N_{T_0} = N_{R_0} = M + K$ and $N_{T_1} = K$. When $K > 1$, an equal power is allocated, i.e., the power of each interference with path loss is $\frac{\tilde{P}_{T_1}}{K}$. As shown in the figure, adaptation of MTIS and AIS achieves the highest SE compared to those fixed IS implementations, whereas STIS yields the lowest SE. Moreover, as K grows, SEs of both non-IM and IS increase, because we set $N_{T_0} = N_{R_0} = M + K$ in the simulation, and hence although a larger K incurs a higher IM cost, the processing gain due to the increase of N_{T_0} and N_{R_0} contributes more to SE. Since non-IM cannot eliminate interference, its SE by employing MF at the PUE improves with $\bar{\gamma}$ in a low $\bar{\gamma}$ region, and saturates at a high $\bar{\gamma}$ with fixed K. As for STIS, its power cost grows as K increases, and its power budget for IS reduces as $\bar{\gamma}$ decreases, i.e., the probability that $\tilde{\mathcal{P}}_{STIS} > P_{T_0}$ grows as K increases and

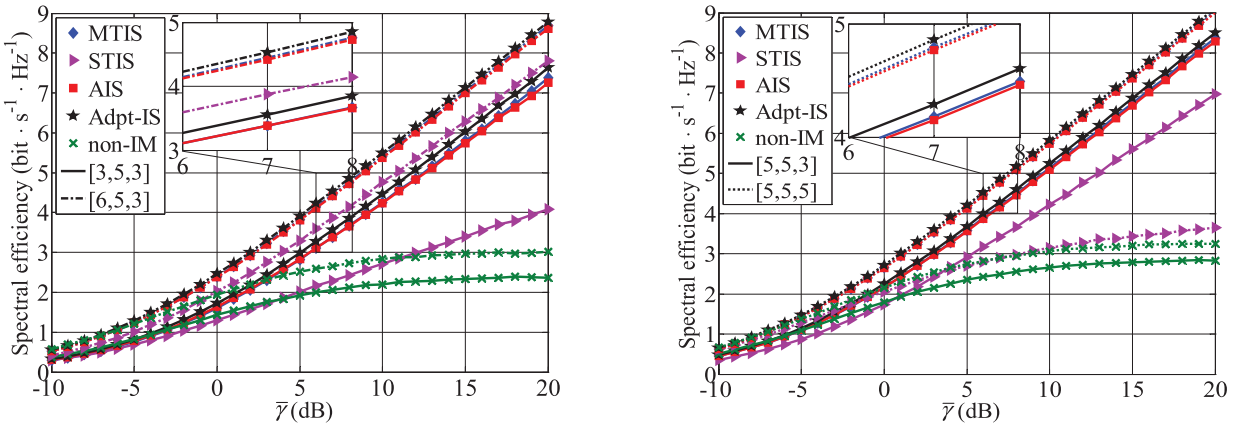

(a) N_{T_0} is variable. (b) N_{R_0} is variable.

Fig. 8. SE of PUE vs. $\bar{\gamma}$ under $\xi = 0.5$ and different antenna settings. (a) N_{T_0} is variable. (b) N_{R_0} is variable.

$\bar{\gamma}$ decreases. Therefore, SE of STIS overlaps with that of non-IM when K is large and $\bar{\gamma}$ is small.

Fig. 8 plots the PUE's average SE along with $\bar{\gamma}$ under $\xi = 0.5$ and different antenna settings. We use a general form $[N_{T_0}, N_{T_1}, N_{R_0}]$ to express the antenna configuration. In Fig. 8(a), N_{T_1} and N_{R_0} are fixed, and N_{T_0} varies from 3 to 6. Since the transmit array gain, related to the number of Tx antennas, of the desired signal grows as N_{T_0} increases, the average SE improves as N_{T_0} increases. When N_{T_0} and N_{R_0} are fixed while varying N_{T_1}, MBS causes random interference to PUE as the PUE uses $\mathbf{f}_0^{(1)}$ to decode $x_0^{(1)}$ regardless of the interference channel matrix $\mathbf{H}_{10}$. Hence, the PUE's average SE under different N_{T_1}s will be similar. Due to space limitation, we omit the results. In Fig. 8(b), N_{T_0} and N_{T_1} are fixed while N_{R_0} varies from 3 to 5. In such antenna settings, the transmit array gain is fixed for both the desired and the interfering signals. As can be seen from the figure, as N_{R_0} grows, the SE of PUE with MTIS and AIS increases monotonically, while STIS's SE increases at low $\bar{\gamma}$, and decreases at medium and high $\bar{\gamma}$ for the following reason. On one hand, as N_{R_0} increases, the receive gain for the intended signal, depending on the filter $\mathbf{f}_0^{(1)}$ — an $N_{R_0} \times 1$ vector designed to match $\mathbf{H}_0$ — grows. As a result, the strength of the desired signal grows as N_{R_0} increases, thus enhancing the PUE's SE. On the other hand, the power cost for different IS schemes (Fig. 9) varies with the increase of N_{R_0}.

As can be seen from Fig. 9, the power consumption of MTIS and AIS is shown to decrease as N_{R_0} increases, hence improving the PUE's SE. However, the STIS's power overhead increases as N_{R_0} increases, thus degrading the SE of PUE. For STIS, as N_{R_0} grows, the decrease of SE incurred by the growing power cost exceeds the increase of SE resulting from the increasing receive gain, therefore behaving in a way opposite to the AIS and MTIS.

Fig. 10 shows the PUE's average SE along with $\bar{\gamma}$ under $\xi = 1$, $K = 2$ and different Ms. Given M desired signals, we set $N_{T_0} = N_{R_0} = M + K$. P_{T_0} is equally allocated to the M data streams. Adpt-IS is shown to outperform the others in terms of SE, STIS yields the lowest SE among the proposed IS-based schemes. In addition, as M grows, more antennas are employed, so that the average SE of different IS schemes

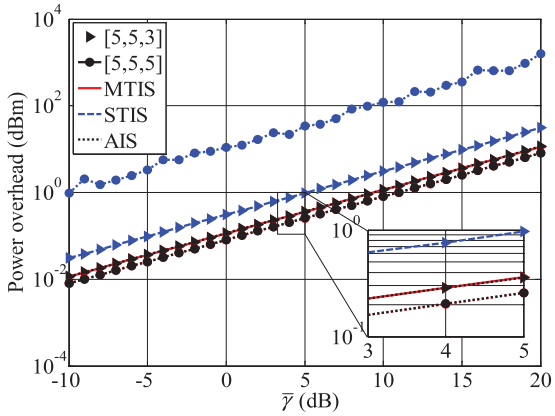

Fig. 9. Power overhead of various IS schemes vs. $\bar{\gamma}$ under $\xi = 0.5$ and different N_{R_0}s.

increases. This is consistent with the results given in Fig. 8(a). Given low $\bar{\gamma}$, SE of non-IM is shown to exceed that of the IS-based schemes, while as $\bar{\gamma}$ grows larger, the IS schemes outperform non-IM in SE. This is because when $\bar{\gamma}$ is low, noise dominates the PUE's SE, and thus the contribution of the IS-based schemes to SE is limited. Moreover, the desired signal's power loss caused by IM degrades the PUE's SE, which may offset the gain of IM.

The authors in [21] generalized the OIS (Orthogonal-IS) [15] to DIS (Dynamic-IS) by introducing a coefficient called *steering factor*, representing the portion of in-phase component of the disturbance to be mitigated, with respect to the desired signal. As presented in [21], DIS outperforms IS by better utilizing the transmit power used for IS and desired signal transmissions. In [21], the average optimal steering factor vs. $\tilde{P}_{T_1}/\sigma_n^2$ (the ratio of transmit power at an interfering transmitter incorporated with path loss to noise, which is similar to $\bar{\gamma}$ defined in this paper, and hence has a similar effect on the simulation results) and different ξ is simulated in Fig. 7. As the figure shows, given fixed ξ, the average optimal steering factor grows with an increase of $\tilde{P}_{T_1}/\sigma_n^2$ (or $\bar{\gamma}$ in this paper). We can also obtain from Fig. 7 in [21] that given the same $\tilde{P}_{T_1}/\sigma_n^2$ (or $\bar{\gamma}$), the average optimal steering factor grows as ξ increases, indicating that larger interference

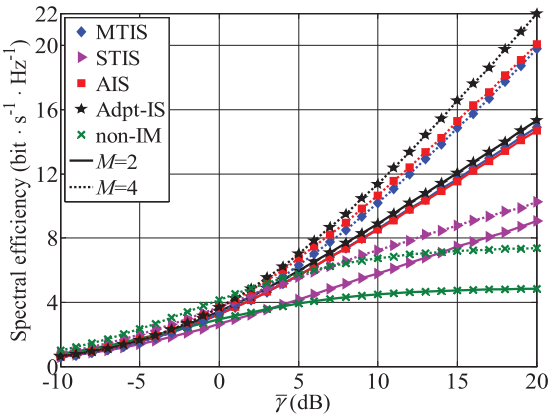

Fig. 10. SE of PUE vs. $\bar{\gamma}$ under $\xi = 1$, $K = 2$ and different Ms.

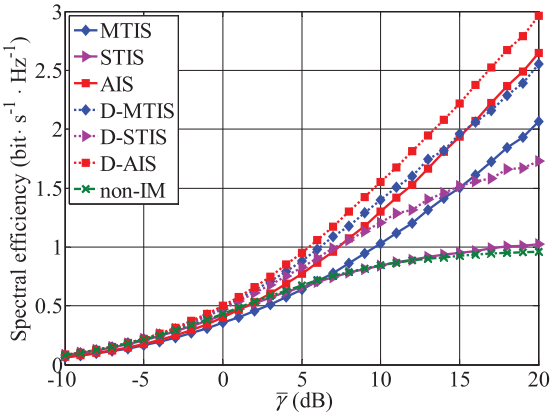

Fig. 11. Comparison of PUE's SE w/ and w/o dynamic transmit power adjustment.

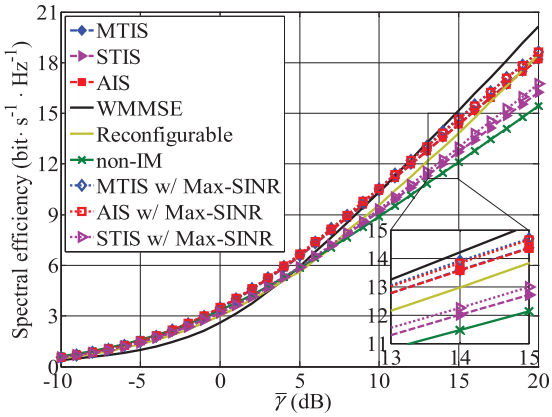

Fig. 12. Comparison of system SE w/ and w/o iterative adjusting the precoder and receive filter under imperfect CSI.

imposed on the desired signal, called the *effective interference*, should be eliminated.

In Fig. 11, PUE's average SE with the proposed IS schemes with and without dynamic transmit power adjustment under $\xi = 0.1$, $K = 2$ disturbances and $N_{T_0} = N_{R_0} = N_{T_1} = 3$ is plotted. The performance of STIS/MTIS/AIS shown in this figure is consistent with that in Fig. 6, so we omit the analysis that can be found in the discussion of Fig. 6. Employing dynamic power adjustment is shown to improve SE of the proposed IS schemes significantly. This is because under $\xi = 0.1$, the power budget for generating steering signal(s) at PBS is very small relative to the strength of interference perceived by the PUE, so the probability of adopting non-IM is high (due to insufficient power for MTIS/STIS/AIS). On the other hand, for the case when MTIS/STIS/AIS is feasible, the optimal amount of power used for generating steering signal(s) with dynamic power allocation is small compared to the traditional orthogonal IS [15], [21], and moreover, by noting that a small optimal steering factor indicates that a small portion of the effective interference should be steered, and based on the results obtained in [21] (see the previous paragraph), orthogonal IS schemes, i.e., MTIS, STIS and AIS, incur a higher unnecessary power cost for interference steering under a small ξ. Therefore, dynamic IS can make a SE gain over orthogonal ones, especially when ξ is small. Therefore, higher power efficiency can be achieved with dynamic implementation of IS, yielding higher SE of D-MTIS/D-STIS/D-AIS than that of MTIS/STIS/AIS. Note that with dynamic MTIS (D-MTIS) and dynamic STIS (D-STIS), the number of steering signals is identical to that of interference. Given $K = 2$, D-MTIS executes the algorithm proposed in [21], whereas for D-STIS, an exhaustive search is employed to find the optimal steering factors.

As for dynamic AIS (D-AIS), since AIS considers the overall effect of multiple interferences, only one steering signal is required. Thus, the operation of D-AIS is similar to that of DIS. As can be seen from the figure, the adoption of dynamic transmit power adjustment improves PUE's SE. The improvement with D-AIS and D-MTIS over AIS and MTIS is moderate compared to that with D-STIS over STIS, especially when $\bar{\gamma}$ is larger, as analyzed below. According to [21], the optimal steering factor decreases as ξ grows. In other words, as the interference grows relatively stronger than the desired signal, IS in [15] incurs a higher unnecessary power cost in steering the interference. Moreover, STIS consumes more power for steering interference than MTIS and AIS. Therefore, D-STIS is more beneficial than D-MTIS and D-AIS from dynamic transmit power adjustment, making a notable SE improvement.

Table III compares IM mechanisms based on signal processing in which the symbols $\surd$ and $\times$ indicate having and not having the corresponding feature, respectively. Two types of communication user-pair are considered: one is the interfered and the other is the interferer. Interfering Tx (Transmitter) beam indicates data transmission from interfering Tx(s). Interfered Rx (Receiver) beam means the direction of the interfered Rx filter's main lobe. Either Tx or Rx beam adjustment will cause effective signal power loss.

Note that ZFBF and IA are not included, because we focus on the adjustment of the interfered transmission pair, while both ZFBF and IA are interfering transmitter-side IM.

Fig. 12 shows the system SE with the proposed IS implementations and their improvements (see Section V-D), as well as WMMSE [38] and the reconfigurable algorithm [39] under $\xi = 0.5$, $N_{T_0} = N_{R_0} = N_{T_1} = 3$ and imperfect CSI. We use the CSI error model given in Eq. (34) and $\rho = 0.95$ [33], [34] as an example to show the effect of imperfect CSI on system SE. What we need to do is to use the erroneous $\widehat{\mathbf{H}}$ instead

TABLE III
COMPARISON OF IM METHODS

Feature \ Method	ZF	IN	IS [15] & DIS [21]	WMMSE [38]	Reconfigurable [39]
Interfering Tx beam adjustment	×	×	×	√	√
Interfered Rx beam adjustment	√	×	×	√	√
Power loss of the interfering user-pair	×	×	×	√	√
Power loss of the interfered user-pair	√	√	√	√	√
Power cost at the interfered Tx-side	×	√	√	×	×
DoF cost at the interfered Rx-side	√	×	√	√	√

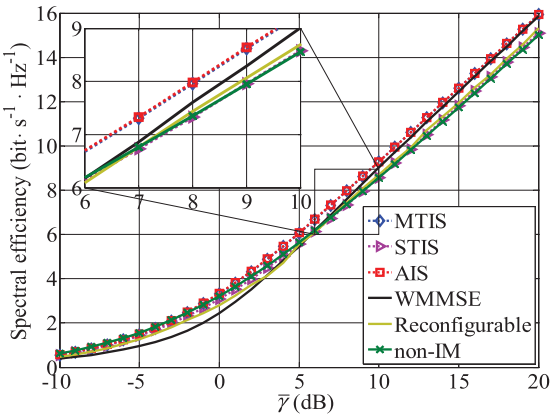

Fig. 13. System SE of various schemes with uncoordinated interference.

of the accurate $\mathbf{H}$ for calculation of the precoding vectors for transmitted data at MBS and PBS, the steering signal(s) at the interfered transmitter, as well as receive filters at the mobile terminals. For simplicity, we omit the subscript 1, 0 or 10 of channel matrices. In particular, all precoders and receive filters are determined based on the erroneous CSI. That is, the channel matrices appearing explicitly or implicitly in the equations related to the determination of steering signal(s), e.g., in Eqs. (3)–(13), (15), (17)–(23), (25), (27)–(29), (33), (35), (38)–(47), etc., should be replaced by the imperfect $\widehat{\mathbf{H}}$. For simplicity, we do not rewrite those equations. As the figure shows, SE of MTIS, STIS and AIS is shown to degrade under imperfect CSI compared to that under perfect CSI (see in Fig. 5(b)). That is, system SE is susceptible to the accuracy of CSI [33], [34]. As for WMMSE, the reconfigurable algorithm and the improved IS schemes (i.e., MTIS/STIS/AIS with Max-SINR), their SE performance is guaranteed by iteratively adjusting precoders and receive filters at the Tx and Rx side, respectively. Moreover, by comparing with Fig. 5(b), their robustness to CSI imperfection is shown to be similar. Although the iterative implementation can improve the robustness of the IM schemes to the CSI error, it may require to exchange signaling information (i.e., precoder and/or receive filter) between the Tx(s) and Rx(s) multiple times, hence impairing their timeliness.

Since WMMSE, reconfigurable algorithm and IS schemes incorporated with Max-SINR operate iteratively, their complexity is determined by the complexity of one iteration and the iteration count. For simplicity, we only discuss the former here. Moreover, these iterative schemes require adjustments at both the interfered and interfering user-pair, while as a comparison, the methods in Table II are interfered transmitter and/or receiver side realizations, so the iterative ones may be more complex.

According to Table I given in [38] and the design of receive filters therein, the complexity of WMMSE is $64N_R^3 + 180N_R^2N_T + 36N_RN_T^2 + 16N_T^3 - 8N_R^2 + 2N_T^2 - 36N_RN_T + 8KN_R^2 + 6N_R + 4N_T - 2KN_R \sim 64N_R^3 + 180N_R^2N_T + 36N_RN_T^2 + 16N_T^3 + 8KN_R^2$. Similarly, the complexity of reconfigurable algorithm can be obtained as $364N_R^3 + 236N_R^2N_T + 36N_RN_T^2 + 16N_T^3 + 8KN_R^2 - 7N_R^2 - 22N_RN_T + 2N_T^2 + 10N_R - 2KN_R + 4N_T \sim 364N_R^3 + 236N_R^2N_T + 36N_RN_T^2 + 16N_T^3 + 8KN_R^2$ based on the Algorithm 1 in [39] and reception design. As for the IS methods incorporated with Max-SINR, their complexity in each iteration can be computed by adding the complexities of two parts: 1) the interfering side complexity incurred by the signal processing at the interfering user-pair given in Section III of this paper, i.e., $48N_R^2N_T + 96N_RN_T^2 + 108N_T^3 + 8KN_R - 8K$, and 2) the complexity due to incorporation of the Max-SINR algorithm presented in [40], i.e., $16N_R^3 + 16N_R^2N_T + 12N_RN_T + 20N_R + 2KN_R$, to the complexity results given in Table II. Since the detailed derivation of the above complexity results is similar to that in Section VI, due to space limit, we omit this.

Fig. 13 plots the system SE of various methods under $\xi = 0.5$, $N_{T_0} = N_{R_0} = N_{T_1} = 3$ and uncoordinated interference which is referred to as OCI in Section V-B. For clarity, perfect CSI is assumed. We model the power of the received aggregate OCI as a Gamma random variable whose strength can be derived as $N_{T_1}\beta\tilde{P}_{T_1}{}^2$ where $\beta \in [0, 1]$ [29]. We set $\beta = 0.2$ in the simulation. As the figure shows, since OCI contributes to an extra disturbance in the denominator of the SINR at the interfered Rx, SE of all schemes gets deteriorated. Given the same β, MTIS and AIS can perform slightly better than WMMSE [38] and the reconfigurable algorithm [39] whereas STIS yields low system SE. This is consistent with the results in Fig. 5(b).

VIII. CONCLUSION

In this paper, we proposed three IS schemes to manage multiple interferences that may originate from one or multiple sources. Of them, MTIS can be regarded as the direct application of traditional IS, STIS is advantageous over MTIS in

[2]For simplicity, we assume all interfering transmitters are equipped with N_{T_1} antennas, have the same power $P_{T_1} = 46$dBm, and experience similar path loss with respect to the interfered receiver.

DoF overhead, whereas by considering the overall effect of multiple interferences, instead of the effect of each interfering signal imposed on the interfered receiver, AIS costs only one DoF regardless of the number of interference. Moreover, AIS consumes the minimum power on the interfered transmitter when the interference signals are destructive with each other. The adaptation of MTIS and AIS can flexibly utilize the power at the interfered transmitter and DoFs at the interfered receiver, and can thus yield the best SE of the interfered transmission pair. Our theoretical analysis and in-depth simulation have shown that the proposed IS schemes can appropriately utilize the DoF and transmit power to manage interference so that the SE of the interfered user-pair can be effectively enhanced.

In this paper, we have considered two types of overhead for IM with different dimensions separately. In practice, however, how to convert the DoF cost to/from the power overhead so as to optimize the interfered user's transmission performance is also an important issue that warrants further investigation. We also considered an asymmetric interference topology, but a symmetric interference model may apply in practice, and hence the extension of IS schemes to such a situation is of practical significance. Moreover, IS relies on transmitter-side cooperation, so building a general model that incorporates the communication scenario studied in this paper and quantizing the cooperation level is useful for investigation of the bound of the proposed schemes. Besides, according to the simulation results, the advantages of IS schemes incorporated with Max-SINR over some existing algorithms in the imperfect CSI situation disappear, so the improved design of the proposed IS methods to combat CSI imperfection is worth a further study. These are the matters of our future inquiry.

Appendices A
Proof of Lemma 1

As shown in Fig. 14, the angle between vectors $\overrightarrow{OA}$ and $\overrightarrow{OB}$ is denoted by $\beta_1 \in (0, \pi)$, whereas that between $\overrightarrow{OA}$ and $\overrightarrow{OC}$ is $\beta_2 \in (0, \pi)$. $\overrightarrow{OB}$ is the orthogonal projection of $\overrightarrow{OA}$ on plane α, i.e., $\overrightarrow{BA} \perp \alpha$, whereas $\overrightarrow{OC}$ is an arbitrary vector lying in α. In solid geometry, the cosine value of β_1 and β_2 can be defined as $\cos\beta_1 = \frac{\langle \overrightarrow{OA}, \overrightarrow{OB} \rangle}{\|\overrightarrow{OA}\|\|\overrightarrow{OB}\|}$ and $\cos\beta_2 = \frac{\langle \overrightarrow{OA}, \overrightarrow{OC} \rangle}{\|\overrightarrow{OA}\|\|\overrightarrow{OC}\|}$, respectively, where $\cos\beta_1$ and $\cos\beta_2$ are real numbers. According to Theorem 1, we have $\cos\beta_1 > \cos\beta_2$. Then,

$$\sin\beta_1 = \cos(\frac{\pi}{2} - \beta_1) < \sin\beta_2 = \cos(\frac{\pi}{2} - \beta_2) \tag{36}$$

is obtained, incurring

$$\|\overrightarrow{OA}\| \sin\beta_1 < \|\overrightarrow{OA}\| \sin\beta_2, \tag{37}$$

thus leading to $\|\overrightarrow{BA}\| < \|\overrightarrow{CA}\|$.

We now let the desired signal $\mathbf{s}$ be perpendicular to the plane α. Since the vectors $\overrightarrow{OB}$ and $\overrightarrow{OC}$ lie in α, they are orthogonal to $\mathbf{s}$. From the comparison with Fig. 2, we adopt $\overrightarrow{OA} = \mathbf{t}^{(k)}$ ($k \in \{1, 2, \ldots, K\}$), and hence $\overrightarrow{OB} = \mathbf{t}^{(k)}_{Q,\perp}$, where $\mathbf{t}^{(k)}_{Q,\perp}$ is the orthogonal projection of $\mathbf{t}^{(k)}$ on α. Similarly, we use $\overrightarrow{OC} = \mathbf{t}^{(k)}_{Q,\angle}$ to denote the non-orthogonal projection of $\mathbf{t}^{(k)}$ on α. When $\mathbf{t}^{(k)}$ is steered to the direction determined by $\overrightarrow{OB}$,

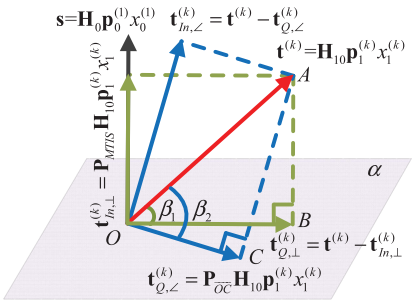

Fig. 14. An illustration of Lemma 1.

the quadrature component of $\mathbf{t}^{(k)}$ is

$$\mathbf{t}^{(k)}_{Q,\perp} = \sqrt{\frac{\tilde{P}_{T_1}}{K}} \mathbf{P}_{\overrightarrow{OB}} \mathbf{H}_{10} \mathbf{p}_1^{(k)} x_1^{(k)}. \tag{38}$$

Otherwise, if $\mathbf{t}^{(k)}$ is adjusted to the direction determined by $\overrightarrow{OC}$, the quadrature component of $\mathbf{t}^{(k)}$ becomes

$$\mathbf{t}^{(k)}_{Q,\angle} = \sqrt{\frac{\tilde{P}_{T_1}}{K}} \mathbf{P}_{\overrightarrow{OC}} \mathbf{H}_{10} \mathbf{p}_1^{(k)} x_1^{(k)}. \tag{39}$$

Here $\mathbf{P}_{\overrightarrow{OB}}$ and $\mathbf{P}_{\overrightarrow{OC}}$ represent for the projection matrices in terms of $\overrightarrow{OB}$ and $\overrightarrow{OC}$, respectively. Recall that $\|\overrightarrow{BA}\| < \|\overrightarrow{CA}\|$, $\|\mathbf{t}^{(k)}_{In,\perp}\| < \|\mathbf{t}^{(k)}_{In,\angle}\|$ can be readily obtained. Thus, we can get $\|\mathbf{t}^{(k)}_{In,\perp}\|^2 < \|\mathbf{t}^{(k)}_{In,\angle}\|^2$.

Based on the above discussion, the power overhead of MTIS for the k^{th} interference can be computed by following Eq. (40):

$$\begin{aligned} P^{(k)}_{MTIS} &= 10^{0.1L_0} \|\mathbf{H}_0^{-1} \mathbf{t}^{(k)}_{In,\perp}\|^2 \\ &= 10^{0.1L_0} [\mathbf{t}^{(k)}_{In,\perp}]^H (\mathbf{H}_0^{-1})^H \mathbf{H}_0^{-1} \mathbf{t}^{(k)}_{In,\perp} \\ &= 10^{0.1L_0} \|\mathbf{H}_0^{-1}\|^2 \|\mathbf{t}^{(k)}_{In,\perp}\|^2. \end{aligned} \tag{40}$$

Similarly, STIS's power cost for the k^{th} interference is

$$P^{(k)}_{STIS} = 10^{0.1L_0} \|\mathbf{H}_0^{-1} \mathbf{t}^{(k)}_{In,\angle}\|^2 = 10^{0.1L_0} \|\mathbf{H}_0^{-1}\|^2 \|\mathbf{t}^{(k)}_{In,\angle}\|^2. \tag{41}$$

By comparing Eq. (40) with Eq. (41), we get $P^{(k)}_{MTIS} < P^{(k)}_{STIS}$, and thus Lemma 1 follows.

Appendices B
Proof of Theorem 2

Recall that the aggregated interference $\mathbf{t}^{(\Sigma)} = \sum_{k=1}^{K} \mathbf{t}^{(k)}$, we can get

$$\mathbf{P}_{AIS} \mathbf{t}^{(\Sigma)} = \mathbf{P}_{MTIS} \sum_{k=1}^{K} \mathbf{t}^{(k)} \tag{42}$$

where $\mathbf{P}_{AIS} = \mathbf{P}_{MTIS}$ denotes the projection matrix with respect to the desired signal $\mathbf{s}$. Since the projection of the interference onto the desired signal is a linear operation,

$$\mathbf{P}_{MTIS} \sum_{k=1}^{K} \mathbf{t}^{(k)} = \sum_{k=1}^{K} [\mathbf{P}_{MTIS} \mathbf{t}^{(k)}] \tag{43}$$

holds, leading to $\mathbf{t}^{(\Sigma)}_{In} = \sum_{k=1}^{K} \mathbf{t}^{(k)}_{In}$, and hence the theorem follows.

APPENDICES C
PROOF OF COROLLARY 1

According to Eqs. (13) and (27), the power overheads of MTIS and AIS are computed as

$$\sum_{k=1}^{K} P_{MTIS}^{(k)} = \sum_{k=1}^{K} \frac{P_{T_1}\varepsilon}{K} \left\| \mathbf{H}_0^{-1}\mathbf{P}_{MTIS}\mathbf{H}_{10}\mathbf{p}_1^{(k)} \right\|^2 = \sum_{k=1}^{K} 10^{0.1L_0} \|\mathbf{H}_0^{-1}\mathbf{t}_{In}^{(k)}\|^2 \quad (44)$$

and

$$P_{AIS}^{(\Sigma)} = \frac{P_{T_1}\varepsilon}{K} \left\| \mathbf{H}_0^{-1}\mathbf{P}_{AIS}[\mathbf{H}_{10}\mathbf{p}_1^{(\hat{k})} + \sum_{k=1,k\neq\hat{k}}^{K} \mathbf{H}_{10}\mathbf{p}_1^{(k)} b_k] \right\|^2 = \frac{P_{T_1}\varepsilon}{K} \|\mathbf{H}_0^{-1}\mathbf{P}_{AIS}\mathbf{E}\|^2 = 10^{0.1L_0} \|\mathbf{H}_0^{-1}\mathbf{t}_{In}^{(\Sigma)}\|^2. \quad (45)$$

Therefore, the comparison of $\sum_{k=1}^{K} P_{MTIS}^{(k)}$ and $P_{AIS}^{(\Sigma)}$ can be replaced by that of $\sum_{k=1}^{K} \|\mathbf{H}_0^{-1}\mathbf{t}_{In}^{(k)}\|^2$ and $\|\mathbf{H}_0^{-1}\mathbf{t}_{In}^{(\Sigma)}\|^2$. Recall that $\mathbf{t}_{In}^{(\Sigma)} = \sum_{k=1}^{K} \mathbf{t}_{In}^{(k)}$, by left multiplying $\mathbf{H}_0^{-1}$ with both side of this equation and exploiting the following relationship,

$$\begin{cases} \mathrm{Re}\{[\mathbf{H}_0^{-1}\mathbf{t}_{In}^{(k)}]^H[\mathbf{H}_0^{-1}\mathbf{t}_{In}^{(k')}]\} = \mathrm{Re}\{[\mathbf{H}_0^{-1}\mathbf{t}_{In}^{(k')}]^H[\mathbf{H}_0^{-1}\mathbf{t}_{In}^{(k)}]\} \\ \mathrm{Im}\{[\mathbf{H}_0^{-1}\mathbf{t}_{In}^{(k)}]^H[\mathbf{H}_0^{-1}\mathbf{t}_{In}^{(k')}]\} = -\mathrm{Im}\{[\mathbf{H}_0^{-1}\mathbf{t}_{In}^{(k')}]^H[\mathbf{H}_0^{-1}\mathbf{t}_{In}^{(k)}]\} \end{cases} \quad (46)$$

where $\mathrm{Re}(\cdot)$ and $\mathrm{Im}(\cdot)$ represent the real and imaginary parts of a complex number. We can obtain

$$\|\mathbf{H}_0^{-1}\mathbf{t}_{In}^{(\Sigma)}\|^2 = \sum_{k=1}^{K} \|\mathbf{H}_0^{-1}\mathbf{t}_{In}^{(k)}\|^2 + 2\sum_{k=1}^{K-1}\sum_{k'=k+1}^{K} \rho_{kk'} = \sum_{k=1}^{K} \|\mathbf{H}_0^{-1}\mathbf{t}_{In}^{(k)}\|^2 + 2\rho_\Sigma \quad (47)$$

where $\rho_{kk'} = \mathrm{Re}\{[\mathbf{H}_0^{-1}\mathbf{t}_{In}^{(k)}]^H[\mathbf{H}_0^{-1}\mathbf{t}_{In}^{(k')}]\}$ indicates the correlation between two disturbances indexed by k and k', $k, k' \in \{1, 2, \ldots, K\}$ and $k \neq k'$. ρ_Σ has impact on the aggregated effect of multiple interferences. When $\rho_\Sigma < 0$, multiple interfering signals destruct with each other, producing a weakened effective interference as compared to $\sum_{k=1}^{K} \|\mathbf{H}_0^{-1}\mathbf{t}_{In}^{(k)}\|^2$. Otherwise, when $\rho_\Sigma > 0$, multiple interferences construct with each other, producing a strengthened equivalent interference at the interfered Rx.

Based on the above analysis, when the spatial features of the K disturbances are positively correlated, we can get $\rho_\Sigma > 0$ and $P_{AIS}^{(\Sigma)} > \sum_{k=1}^{K} P_{MTIS}^{(k)}$. Otherwise, when they are negatively correlated, $\rho_\Sigma < 0$ and $P_{AIS}^{(\Sigma)} < \sum_{k=1}^{K} P_{MTIS}^{(k)}$ are obtained. Therefore, Corollary 1 is proved.

REFERENCES

[1] T. Yoo and A. Goldsmith, "On the optimality of multiantenna broadcast scheduling using zero-forcing beamforming," *IEEE J. Sel. Areas Commun.*, vol. 24, no. 3, pp. 528–541, Mar. 2006.

[2] D. Tse and P. Viswanath, *Fundamentals of Wireless Communication*. Cambridge, U.K.: Cambridge Univ. Press, 2004.

[3] C. M. Yetis, T. Gou, S. A. Jafar, and A. H. Kayran, "On feasibility of interference alignment in MIMO interference networks," *IEEE Trans. Signal Process.*, vol. 58, no. 9, pp. 4771–4782, Sep. 2010.

[4] S. A. Jafar and S. Shamai (Shitz), "Degrees of freedom region of the MIMO X channel," *IEEE Trans. Inf. Theory*, vol. 54, no. 1, pp. 151–170, Jan. 2008.

[5] M. A. Maddah-Ali, A. S. Motahari, and A. K. Khandani, "Communication over MIMO X channels: Interference alignment, decomposition, and performance analysis," *IEEE Trans. Inf. Theory*, vol. 54, no. 8, pp. 3457–3470, Aug. 2008.

[6] V. R. Cadambe and S. A. Jafar, "Interference alignment and degrees of freedom of the K-user interference channel," *IEEE Trans. Inf. Theory*, vol. 54, no. 8, pp. 3425–3441, Aug. 2008.

[7] C. Suh, M. Ho, and D. N. C. Tse, "Downlink interference alignment," *IEEE Trans. Commun.*, vol. 59, no. 9, pp. 2616–2626, Sep. 2011.

[8] Z. Li, K. G. Shin, and L. Zhen, "When and how much to neutralize interference?" in *Proc. IEEE Conf. Comput. Commun. (INFOCOM)*, May 2017, pp. 1–9.

[9] J. Chen, A. Singh, P. Elia, and R. Knopp, "Interference neutralization for separated multiuser uplink-downlink with distributed relays," in *Proc. Inf. Theory Appl. Workshop*, Feb. 2011, pp. 1–9.

[10] J. Zhang, Z. K. M. Ho, E. Jorswieck, and M. Haardt, "SINR balancing for non-regenerative two-way relay networks with interference neutralization," in *Proc. IEEE Int. Conf. Acoust., Speech Signal Process. (ICASSP)*, May 2014, pp. 7604–7608.

[11] D. Wu, C. Yang, T. Liu, and Z. Xiong, "Feasibility conditions for interference neutralization in relay-aided interference channel," *IEEE Trans. Signal Process.*, vol. 62, no. 6, pp. 1408–1423, Mar. 2014.

[12] T. Gou *et al.*, "Aligned interference neutralisation for $2 \times 2 \times 2$ interference channel with imperfect channel state information," *IEEE Trans. Inf. Theory*, vol. 58, no. 7, pp. 4381–4395, Mar. 2012.

[13] Z. K. M. Ho and E. A. Jorswieck, "Instantaneous relaying: Optimal strategies and interference neutralization," *IEEE Trans. Signal Process.*, vol. 60, no. 12, pp. 6655–6668, Dec. 2012.

[14] N. Lee and C. Wang, "Aligned interference neutralization and the degrees of freedom of the two-user wireless networks with an instantaneous relay," *IEEE Trans. Commun.*, vol. 61, no. 9, pp. 3611–3619, Sep. 2013.

[15] Z. Li *et al.*, (2017)."Interference steering to manage interference." Accessed: Mar. 21, 2019. [Online]. Available: https://arxiv.org/abs/1712.07810

[16] C.-B. Chae, D. Mazzarese, N. Jindal, and R. W. Heath, "Coordinated beamforming with limited feedback in the MIMO broadcast channel," *IEEE J. Sel. Areas Commun.*, vol. 26, no. 8, pp. 1505–1515, Oct. 2008.

[17] V. Raghavan, S. V. Hanly, and V. V. Veeravalli, "Statistical beamforming on the Grassmann manifold for the two-user broadcast channel," *IEEE Trans. Inf. Theory*, vol. 59, no. 10, pp. 6464–6489, Oct. 2013.

[18] M. Dai and B. Clerckx, "Transmit beamforming for MISO broadcast channels with statistical and delayed CSIT," *IEEE Trans. Commun.*, vol. 63, no. 4, pp. 1202–1215, Apr. 2015.

[19] J. Choi, V. Raghavan, and D. J. Love, "Limited feedback design for the spatially correlated multi-antenna broadcast channel," in *Proc. IEEE Global Commu Conf. (GLOBECOM)*, Dec. 2013, pp. 3481–3486.

[20] V. Raghavan, J. J. Choi, and D. J. Love, "Design guidelines for limited feedback in the spatially correlated broadcast channel," *IEEE Trans. Commun.*, vol. 63, no. 7, pp. 2524–2540, Jul. 2015.

[21] Z. Li, F. Guo, C. Shu, Kang G. Shin, and J. Liu, "Dynamic interference steering in heterogeneous cellular networks," *IEEE Access*, vol. 6, pp. 28552–28562, May 2018.

[22] T. Q. S. Quek, G. de la Roche, and M. Kountouris, *Small Cell Networks: Deployment, PHY Techniques, and Resource Management*. Cambridge, U.K: Cambridge Univ. Press, 2013.

[23] *LTE; Evolved Universal Terrestrial Radio Access (E-UTRA); Radio Frequency (RF) Requirements for LTE Pico Node B*, document 3GPP TR36.931 Release 14, 2017.

[24] Cisco, "Cisco visual networking index: Global mobile data traffic forecast update, 2017-2022," White Paper, 2019. Accessed: Apr. 16, 2019. [Online]. Available: https://www.cisco.com/c/en/us/solutions/collateral/service-provider/visual-etworking-index-vni/white-paper-c11-738429.pdf

[25] F. Pantisano, M. Bennis, W. Saad, M. Debbah, and M. Latva-Aho, "Interference alignment for cooperative femtocell networks: A game-theoretic approach," *IEEE Trans. Mobile Comput.*, vol. 12, no. 11, pp. 2233–2246, Nov. 2013.

[26] H. Sun, "Application of the minimum angle theorem," *Math. Commun.*, vol. 1, p. 10, Jan. 1999.

[27] Z. Li, X. Dai, and K. G. Shin, "Decoding interfering signals with fewer receiving antennas," in *Proc. 35th Annu. IEEE Int. Conf. Comput. Commun.*, Apr. 2016, pp. 1–9.

[28] G. C. Alexandropoulos, P. Ferrand, J.-M. Gorce, and C. B. Papadias, "Advanced coordinated beamforming for the downlink of future LTE cellular networks," *IEEE Commun. Mag.*, vol. 54, no. 7, pp. 54–60, Jul. 2016.
[29] G. C. Alexandropoulos, P. Ferrand, and C. B. Papadias, "On the robustness of coordinated beamforming to uncoordinated interference and CSI uncertainty," in *Proc. IEEE Wireless Commun. Netw. Conf. (WCNC)*, Mar. 2017, pp. 1–6.
[30] R. F. Ustok, P. A. Dmochowski, P. J. Smith, and M. Shafi, "Interference cancellation with jointly optimized transceivers in multiuser multicellular networks," *IEEE Trans. Veh. Technol.*, vol. 67, no. 8, pp. 7219–7229, Aug. 2018.
[31] A. Lozano, R. W. Heath, and J. G. Andrews, "Fundamental limits of cooperation," *IEEE Trans. Inf. Theory*, vol. 59, no. 9, pp. 5213–5226, Sep. 2013.
[32] O. El Ayach, "Interference alignment from theory to practice," Ph.D. dissertation, ECE, Univ. Texas, Austin, TX, USA, 2013.
[33] R. F. Ustok, P. A. Dmochowski, P. J. Smith, and M. Shafi, "Aligned interference neutralisation for $2 \times 2 \times 2$ interference channel with imperfect channel state information," in *Proc. IEEE Int. Conf. Commun. (ICC)*, Jun. 2013, pp. 5230–5235.
[34] R. F. Ustok, P. A. Dmochowski, P. J. Smith, and M. Shafi, "Cooperative interference cancellation for cellular networks with imperfect CCSI," *IET Commun.*, vol. 10, no. 5, pp. 525–533, Apr. 2016.
[35] L. Tong, B. M. Sadler, and M. Dong, "Pilot-assisted wireless transmissions: General model, design criteria, and signal processing," *IEEE Signal Process. Mag.*, vol. 21, no. 6, pp. 12–25, Nov. 2004.
[36] K. S. Ahn and R. W. Heath, "Performance analysis of maximum ratio combining with imperfect channel estimation in the presence of cochannel interferences," *IEEE Trans. Wireless Commun.*, vol. 8, no. 3, pp. 1080–1085, Mar. 2009.
[37] Q. Sun, D. C. Cox, H. C. Huang, and A. Lozano, "Estimation of continuous flat fading MIMO channels," *IEEE Trans. Wireless Commun.*, vol. 1, no. 4, pp. 549–553, Dec. 2002.
[38] Q. Shi, M. Razaviyayn, Z.-Q. Luo, and C. He, "An iteratively weighted MMSE approach to distributed sum-utility maximization for a MIMO interfering broadcast channel," *IEEE Trans. Signal Process.*, vol. 59, no. 9, pp. 4331–4340, Sep. 2011.
[39] G. C. Alexandropoulos and C. B. Papadias, "A reconfigurable iterative algorithm for the K-user MIMO interference channel," *Signal Process.*, vol. 93, no. 12, pp. 3353–3362, Dec. 2013.
[40] K. Gomadam, V. R. Cadambe, and S. A. Jafar, "A distributed numerical approach to interference alignment and applications to wireless interference networks," *IEEE Trans. Inf. Theory*, vol. 57, no. 6, pp. 3309–3322, Jun. 2011.
[41] J. P. Kermoal, L. Schumacher, K. I. Pedersen, P. E. Mogensen, and F. Frederiksen, "A stochastic MIMO radio channel model with experimental validation," *IEEE J. Sel. Areas Commun.*, vol. 20, no. 6, pp. 1211–1226, Aug. 2002.
[42] D.-S. Shiu, G. J. Foschini, M. J. Gans, and J. M. Kahn, "Fading correlation and its effect on the capacity of multielement antenna systems," *IEEE Trans. Commun.*, vol. 48, no. 3, pp. 502–513, Mar. 2000.
[43] G. H. Golub and C. F. Van Loan, *Matrix Computations*, 4th ed. Baltimore, MD, USA: John Hopkins Univ. Press, 2013.
[44] J. H. Lee and W. Choi, "Interference alignment by opportunistic user selection in 3-user MIMO interference channels," in *Proc. IEEE ICC*, Jun. 2011, pp. 1–5.

Zhao Li (S'08–M'10) received the B.S. degree in telecommunications engineering and the M.S. and Ph.D. degrees in communication and information systems from Xidian University, Xi'an, China, in 2003, 2006, and 2010, respectively. He was a Visiting Scholar and then a Research Scientist with the Real-Time Computing Laboratory, Department of Electrical Engineering and Computer Science, The University of Michigan, from 2013 to 2015. He is currently an Associate Professor with the School of Cyber Engineering, Xidian University. He is also with the Shaanxi Key Laboratory of Information Communication Network and Security, Xi'an University of Posts and Telecommunications, and School of Information Engineering, Eurasia University. He has published over 40 technical papers at premium international journals and conferences, including the IEEE TWC, the IEEE INFOCOM, and *Computer Communications*. His research interests include wireless communications, 5G communication systems, resource allocation, interference management, the IoT, and physical layer security.

Yinghou Liu is currently pursuing the master's degree with the School of Telecommunications Engineering, Xidian University. His research interests include wireless communication, resource allocation, and interference management.

Kang G. Shin (LF'12) received the B.S. degree in electronics engineering from Seoul National University, Seoul, South Korea, and the M.S. and Ph.D. degrees in electrical engineering from Cornell University, Ithaca, NY, USA, in 1970, 1976, and 1978, respectively. He is the Kevin and Nancy O'Connor Professor of computer science and the Founding Director of the Real-Time Computing Laboratory, Department of Electrical Engineering and Computer Science, The University of Michigan, Ann Arbor, MI, USA. At Michigan, he has supervised the completion of 82 Ph.D. students. From 1978 to 1982, he was a Faculty Member of the Rensselaer Polytechnic Institute, Troy, NY, USA. He has authored or coauthored over 900 technical articles (more than 330 of which are published in archival journals). He holds more than 30 patents or invention disclosures. His current research interests focus on QoS-sensitive computing and networks, and embedded real-time and cyber-physical systems. He was the Chair of the Computer Science and Engineering Division for 3 years starting in 1991. He has also received numerous institutional awards and the best paper awards. He is a fellow of the ACM.

Jun Li is currently pursuing the master's degree with the School of Cyber Engineering, Xidian University. Her research interests include wireless communication, resource allocation, and interference management.

Fengjuan Guo is currently pursuing the master's degree with the School of Telecommunications Engineering, Xidian University. Her research interests include wireless communication, resource allocation, and interference management.

Jia Liu (S'10–M'12) received the Ph.D. degree from the School of Systems Information Science, Future University Hakodate, Japan, in 2016. He is currently an Assistant Professor with the Center for Cybersecurity Research and Development, National Institute of Informatics, Japan. His research interests include mobile ad hoc networks, 5G communication systems, D2D communications, the IoT, physical layer security, and cyber security. He has published over 20 technical papers at premium international journals and conferences, such as the IEEE TWC, the IEEE TVT, the IEEE INFOCOM, and *Computer Networks*. He has received the 2016 IEEE Sapporo Section Encouragement Award and the Best Paper Award from NaNA 2017.